

Master Thesis



Czech  
Technical  
University  
in Prague

**F3**

Faculty of Electrical Engineering  
Department of Control Engineering

## Advanced traction system development

**Bc. Jakub Valerián**

Supervisor: doc. Ing. Tomáš Haniš, Ph.D.

Supervisor–specialist: Ing. Juraj Madarás, Ph.D.

August 2021



## Acknowledgements

Rád bych poděkoval svému vedoucímu za trpělivost a čas při konzultacích a také za připomínky a asistenci při řešení diplomové práce.

Zároveň bych rád poděkoval svým kolegům a nadřízeným z Porsche Engineering Services, Ing. Martinu Řezáčovi, Ph.D., a Ing. Juraji Madarásovi, Ph.D., za návrh tématu práce, připomínky k realizaci vzhledem k přístupu z průmyslové strany.

V neposlední řadě bych chtěl poděkovat také spolužákům a pracovníkům fakulty za linearizační nástroj, týmu ČVUT e-formule za poskytnutí jejich vývojového modelu pro testování a firmě IPG za poskytnutí licence k softwaru Carmaker.

Nakonec moje poděkování patří i mojí rodině a přátelům za pochopení a (nejenom) morální podporu při vypracovávání této práce, ale i po dobu mého studia.

I would like to thank my supervisor for his support and time spent on the consultations and for many inspiring comments.

Also, I would like to thank my colleagues and superiors from Porsche Engineering Services, namely to Ing. Martin Řezáč, Ph.D, and Ing. Juraj Madarás, Ph.D., for the proposal of the thesis topic and comments to the realization.

Another thanks goes to my classmates and university employees for the linearization tool, to the CTU e-formula team for letting me use their development model for testing, and to the IPG company for providing the licence to their Carmaker product.

Last but not least, I would like to thank my family and friends for understanding and (not only) moral support during not only during the thesis development, but during all my studies.

## Declaration



Prohlašuji, že jsem předloženou práci vypracoval samostatně, a že jsem uvedl veškerou použitou literaturu.

V Praze, 12. srpna 2021

## Abstract

This thesis focuses on the design of an advanced traction control system for an electric vehicle. The first part is dedicated to the theoretical research where the vehicle propulsion is described and relation between the tire and the traction force is discussed. Then the differences between the electric vehicles and a regular internal combustion engine vehicles are described and the necessity of different control approach is pointed out. In the second part the model for the controller design is defined with the Model Predictive Control, which was used for the controller prototype in the simulated environment. The last part is dedicated to the discussion of the results of the testing and suggests possible further improvements to the developed control.

**Keywords:** traction control system, model predictive control, torque vectoring, electric vehicles

**Supervisor:** doc. Ing. Tomáš Haniš,  
Ph.D.  
ČVUT FEL  
Katedra řídicí techniky  
Karlovo náměstí 13  
Praha

## Abstrakt

Tato práce pojednává o návrhu pokročilé trakční kontroly pro elektrické vozidlo. První část je věnována teoretickému průzkumu, tedy pohonu celého vozidla a přenosu síly přes pneumatiky, jednotlivým typům elektrických vozidel a porovnání s klasickými vozidly se spalovacím motorem. Je ukázáno, proč je potřeba pro určitá vozidla, pohonem podobná vozidlu v této práci, přijít s novým konceptem pro trakční kontrolu. Druhá část se věnuje podrobněji použitému modelu a principu 'model predictive control' použitému v návrhu řízení a jeho konkrétní implementaci v simulovaném prostředí. Třetí část poté interpretuje dosažené výsledky a závěrem konstatuje možnou budoucí směry rozšíření stávajícího systému.

**Klíčová slova:** kontrola trakce, model predictive control, torque vectoring, elektrická vozidla

**Překlad názvu:** Návrh pokročilého trakčního systému vozu

# Contents

|   |           |  |  |
|---|-----------|--|--|
| <b>1 Introduction</b>   | <b>1</b>  |  |  |
| 1.1 Abbreviations, quantities and symbols                                 | 2         |  |  |
| <b>2 Electric and internal combustion engine vehicle</b>                  | <b>3</b>  |  |  |
| 2.1 Electric and internal combustion engine vehicle powertrain comparison | 3         |  |  |
| 2.1.1 ICE Drivetrain  | 4         |  |  |
| 2.1.2 Hybrid vehicles   | 4         |  |  |
| 2.1.3 Electric vehicles powertrain  | 6         |  |  |
| 2.2 Tractive force  | 7         |  |  |
| <b>3 Vehicle control systems</b>  | <b>9</b>  |  |  |
| 3.1 A general overview  | 9         |  |  |
| 3.2 Traction control system   | 11        |  |  |
| 3.2.1 Functionality   | 11        |  |  |
| 3.2.2 Algorithms  | 12        |  |  |
| 3.3 Torque vectoring  | 13        |  |  |
| 3.3.1 Understeering, oversteering and a neutral vehicle                   | 14        |  |  |
| 3.3.2 Current torque vectoring systems                                    | 15        |  |  |
| <b>4 Mathematical models</b>  | <b>17</b> |  |  |
| 4.1 Mathematical model of the vehicle                                     | 17        |  |  |
| 4.1.1 Dual track vehicle model  | 18        |  |  |
| 4.1.2 Wheel model   | 20        |  |  |
| 4.2 Design model and verification   | 23        |  |  |
| 4.3 External conditions model   | 25        |  |  |
| <b>5 Control design</b>   | <b>27</b> |  |  |
| 5.1 Performance requirements  | 27        |  |  |
| 5.1.1 Vehicle performance requirements                                    | 28        |  |  |
| 5.1.2 Scenarios   | 30        |  |  |
| 5.2 Control development   | 32        |  |  |
| 5.2.1 Assumptions, simplifications and limitations                        | 32        |  |  |
| 5.2.2 Model Predictive Control  | 34        |  |  |
| 5.3 Implementation  | 36        |  |  |

|  |           |
|--|-----------|
| <b>6 Verification and testing</b>              | <b>39</b> |
| 6.1 Testing with the high fidelity model ..... | 39        |
| 6.1.1 Acceleration maneuver .....              | 41        |
| 6.1.2 Cornering .....                          | 43        |
| 6.2 Testing in IPG Carmaker .....              | 45        |
| 6.2.1 Acceleration maneuver .....              | 46        |
| 6.2.2 Cornering .....                          | 49        |
| <b>7 Conclusion</b>                            | <b>53</b> |
| 7.1 Results .....                              | 53        |
| 7.2 Future work .....                          | 54        |
| <b>A Bibliography</b>                          | <b>55</b> |
| <b>B Project specification</b>                 | <b>59</b> |
| <b>C CD Contents</b>                           | <b>61</b> |

## Figures

|  |  |
|--|--|
| <p>2.1 A principle scheme of a typical ICE powertrain; picture adopted from [2] 4</p> <p>2.2 An example of a parallel hybrid vehicle architecture as implemented in BMW 740e; picture adopted from [5]. Legend: 1 - ICE, 2 - Engine disconnect clutch, 3 - Electric machine, 4 - Automatic transmission, 5 - Power electronics, 6 - High voltage battery, 7 - Rear differential 5</p> <p>2.3 An example of EV using one motor on each wheel - Rimac Concept_one; picture adopted from [4] ..... 6</p> <p>2.4 A concept chassis for an EV with one motor per wheel, solution used in Tesla Model S; picture adopted from [6] ..... 7</p> <p>3.1 An example of the ESP system in use; picture adopted from [17] .... 10</p> <p>3.2 Tractive force based on Pacejka's magic formula ..... 11</p> <p>3.3 An example of TV, cornering maneuver; picture adopted from [7] 13</p> <p>3.4 An example of behavior of an understeering, oversteering and neutral (pictured as <i>desired course</i>) vehicle adopted from [2]. The figure shows a possible solution adopted from the ESP when brake pressure is applied to slow the inner or outer wheel to achieve neutral steer. .... 14</p> | <p>3.5 Dependency of the steering angle <math>\delta</math> on longitudinal velocity <math>V_x</math> for all types of steering; adopted from [11] .... 15</p> <p>4.1 Two principle vehicle coordinate system; picture adopted from [2] .. 18</p> <p>4.2 A simple vehicle scheme showing coefficients associated to wheels positions..... 20</p> <p>4.3 An example of Kamm's (friction) circle ..... 22</p> <p>4.4 An example of split <math>\mu</math> road on a testing site; picture taken from [16] 23</p> <p>4.5 Doublet source signal ..... 24</p> <p>4.6 Verification of the linear model, response to doublet signal on the steering wheel ..... 24</p> <p>5.1 An example scenario for acceleration and cornering at the same time with velocity references along the trajectory. Designed in Matlab's Driving Scenario Designer. 32</p> <p>5.2 An example scenario of a long turn with possible split <math>\mu</math>. Designed in Matlab's Driving Scenario Designer. 33</p> <p>5.3 Control scheme ..... 34</p> |
|--|--|



|  |    |  |    |
|--|----|--|----|
| 6.1 Wheels rotation rates in uncontrolled simulation setup on split $\mu$ road.....  | 40 | 6.10 Cornering during acceleration on split $\mu$ road, wheels rotation rates for the left wheel in the upper figure, right wheel is in the lower part....         | 45 |
| 6.2 Yaw rate in uncontrolled simulation on split $\mu$ road.....   | 40 | 6.11 CTU e-formula model in IPG Carmaker .....   | 46 |
| 6.3 Nonlinear model implemented in Simulink.....   | 41 | 6.12 Control algorithm integrated into the Carmaker model .....  | 46 |
| 6.4 Response of the controlled system to the acceleration and deceleration. Fluctuations during the acceleration appeared due to reaching omega limit.....   | 42 | 6.13 Velocity reference calculation from brake and acceleration pedal signals  | 47 |
| 6.5 Response of the controlled system to the acceleration and deceleration; wheel rotation rates. Left wheel rotation rates and limit are displayed in the upper plot, the right in the lower one..... | 42 | 6.14 Motor torques during the acceleration .....   | 47 |
| 6.6 Response of the controlled system to the acceleration and deceleration on split $\mu$ road. Upper part displays the left wheel behaviour, the right one is in the lower part. ....                 | 43 | 6.15 Controlled system response to acceleration, velocity .....  | 48 |
| 6.7 Response of the controlled system to the acceleration and deceleration on split $\mu$ road; wheels rotation rates .....  | 43 | 6.16 Controlled system response to acceleration, wheels rotation rates. The left wheel behaviour is in the upper plot, the lower plot is for the right wheel. .... | 48 |
| 6.8 Response of the system to acceleration and cornering - velocity and yaw rate .....   | 44 | 6.17 Controlled system response to acceleration on split $\mu$ road .....  | 49 |
| 6.9 Response of the system to acceleration and cornering on split $\mu$ road, yaw rate and torques .....   | 44 | 6.18 Controlled system response to acceleration on split $\mu$ road, wheels rotation rates - left wheel in the upper plot, right wheel in the lower plot. ....     | 49 |
|  |    | 6.19 Carmaker simulation results, open loop cornering test .....   | 50 |
|  |    | 6.20 Simulation of acceleration into a turn.....   | 50 |

|  |    |
|--|----|
| 6.21 Simulation of acceleration into a double lane change maneuver, velocity and yaw rate..... | 51 |
| 6.22 Simulation of acceleration into a turn, wheels rotation rates and torques .....           | 51 |
| 6.23 Simulation of acceleration into a long turn .....   | 52 |

## Tables

|   |    |
|---|----|
| 1.1 List of abbreviations .....   | 2  |
| 1.2 List of quantities and constants with the respective units .....  | 2  |
| 3.1 Values of understeering coefficient and how it indicates the slip angles relation for front ( $\alpha_f$ ) and rear ( $\alpha_r$ ) wheel [11] ..... | 15 |
| 4.1 Values of $\mu$ for various road surfaces; based on Buckhardt as stated in [2] .....  | 21 |



# Chapter 1

## Introduction

Driving a car or being a passenger in one is an everyday part of many people's lives. During the last several decades the mankind had witnessed not only a growing number of road vehicles, but also technical advances in the field of vehicle technology. Combined with more accessible and affordable computational power and sensors, the autonomous cars are being developed and apart of that the performance and safety of the vehicles can be improved.

Several advanced driver-assistance systems (ADAS) have been designed and implemented until now, for example parking sensors or assistants which can autonomously perform minor maneuvers such as parking, cruise control with keeping the distance from the vehicle in front or keeping the given speed, stability assistants and many more. In case of autonomous cars, the development went even further.

This thesis is focused on the traction control system (TCS) and torque vectoring (TV) as designed for an electric vehicle (EV), namely the rear drive using one motor on each rear wheel. In the introductory first part, the power transmission in a vehicle is described together with differences between a vehicle with an internal combustion engine (ICE) and an EV. The TCS and TV is defined and existing solutions are presented for both types of the mentioned propulsion systems. In the second part the framework used for development is described and the controller design is presented followed by the description of implementation. In the last, third part the results of the testing in simulated environment is described with proposed future development.

## 1.1 Abbreviations, quantities and symbols

Abbreviations, quantities, constants and their respective units used in the work are listed below.

| Abbreviation | Full name                    |
|--------------|------------------------------|
| ICE          | Internal Combustion Engine   |
| EV           | Electric Vehicle             |
| TCS          | Traction Control System      |
| ABS          | Antilock Braking System      |
| ESP          | Electronic Stability Program |
| TV           | Torque Vectoring             |
| FR(L)        | Front Right (Left)           |
| RR(L)        | Rear Right (Left)            |
| MPC          | Model Predictive Control     |
| CoG          | Center of Gravity            |

**Table 1.1:** List of abbreviations

| Symbol       | Quantity                                  | Unit             |
|--------------|---|------------------|
| $\beta$      | Side slip angle                           | rad              |
| $\psi$       | Yaw angle                                 | rad              |
| $\mu$        | Road friction coefficient                 | -                |
| $\lambda$    | Wheel slip ratio                          | -                |
| $\alpha$     | Wheel slip angle                          | rad              |
| $\omega$     | Wheel rotation rate                       | deg              |
| r            | Wheel radius = 0.195                      | m                |
| v            | Velocity                                  | ms <sup>-1</sup> |
| L            | Wheelbase = 1.53                          | m                |
| J            | Wheel moment of inertia = 0.13            | kgm <sup>2</sup> |
| $\delta$     | Steering angle                            | rad              |
| tr           | Vehicle track                             | m                |
| $\phi_{f,r}$ | Angle between the CoG to front/rear wheel | rad              |
| $p_{f,r}$    | Distance from CoG to front/rear wheel     | m                |
| $I_z$        | Vehicle moment of inertia = 120           | kgm <sup>2</sup> |

**Table 1.2:** List of quantities and constants with the respective units




## Chapter 2

### Electric and internal combustion engine vehicle

The ICE vehicles are being developed and used for significantly longer market penetration than the EVs. The drivetrains in both vehicles might differ in several ways and some major differences might require different approach in terms of control.

In this chapter, the general power transmission common for all road vehicles is described. Then the major differences between an EV and an ICE vehicle and their consequences for the control approach are reviewed together with their advantages and disadvantages.



#### 2.1 Electric and internal combustion engine vehicle powertrain comparison

There are several differences between the powertrain of an EV and an ICE vehicle apart from the power source. This section describes briefly the ICE vehicle, types of hybrid vehicles and EVs and the differences between them from the control point of view as the control approach differ for each of them.

### 2.1.1 ICE Drivetrain

The conventional drivetrain of an ICE vehicle is shown in figure 2.1. The engine is connected to a clutch followed by a transmission. The transmission is then followed by a final drive which connects to wheels.

The final drive, usually in a form of a differential, distributes the torque between wheels while compensating the differences between rotation rates during cornering maneuvers [3]. This is common to all differentials. A more advanced solution is a limited slip differential which is able to limit torque on one wheel by increasing the friction inside the differential. The last differential is the torque vectoring differential. Among the mentioned final drives, it is the most complicated solution actively using electronic sensors and redistributing inequally torques to wheels to generate the yaw torque.

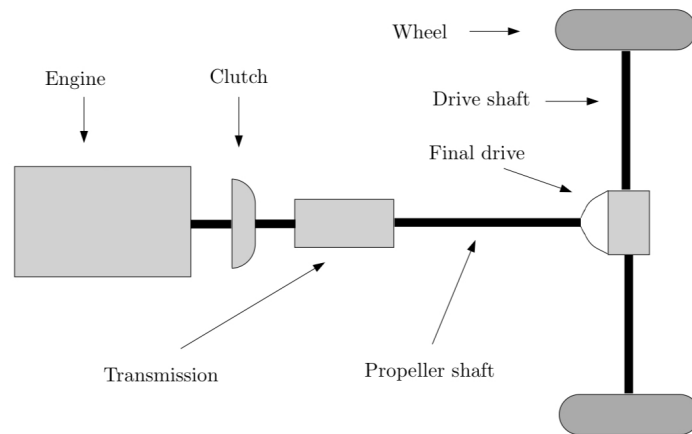


**Figure 2.1:** A principle scheme of a typical ICE powertrain; picture adopted from [2]

### 2.1.2 Hybrid vehicles

Between an ICE vehicle and an EV, there is a class of hybrid vehicles. There are several types of realizations of hybrids. The hybrid vehicles can benefit from both propulsion advantages, among others:

- faster response of the electric motor - electric motor can boost the vehicle on acceleration with minimum delay;
- an electric motor does not have any  $\text{CO}_x$  exhaust gases in the place of usage;

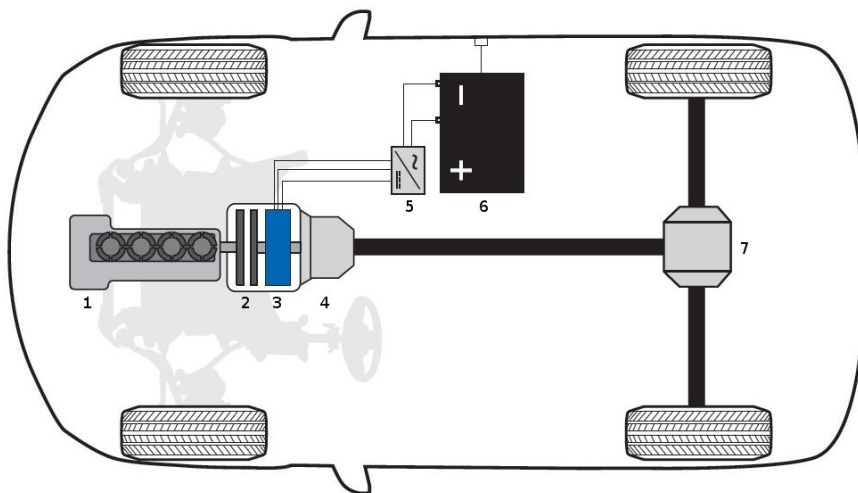


**Figure 2.2:** An example of a parallel hybrid vehicle architecture as implemented in BMW 740e; picture adopted from [5]. Legend: 1 - ICE, 2 - Engine disconnect clutch, 3 - Electric machine, 4 - Automatic transmission, 5 - Power electronics, 6 - High voltage battery, 7 - Rear differential

- an ICE performs better on longer trips where the EV's battery might need to be recharged more than once while the EV is more suitable on shorter distances;
- refueling is faster than recharging, even with a fast charging station;
- the hybrid vehicle is able to recuperate energy from brakes, not only from chargers or the engine.

Also, on shorter trips the hybrid can drive solely with the electric motor which can be more effective.

The hybrid vehicles differ by both the electric motor connection and the recharging of the batteries. In a parallel hybrid car, the wheels can be powered by the ICE, electric motor or both at the same time (an example is displayed in figure 2.2). There can be one motor for each wheel or only one motor for two (or all) powered wheels. The torque is then again transmitted through the final drive unit. Other possibility is to mount one motor to each powered wheel which allows better control over the wheel rotation rates with a final drive without TV feature. The last type of hybrid vehicle is the vehicle with serial connection of the electric motor and the engine where the ICE serves as the power source for the electric motor. The wheels are then never powered by the ICE directly, only via electric motors. The series hybrid vehicle is the closest to the full EV as the propulsion is purely electric.

### 2.1.3 Electric vehicles powertrain

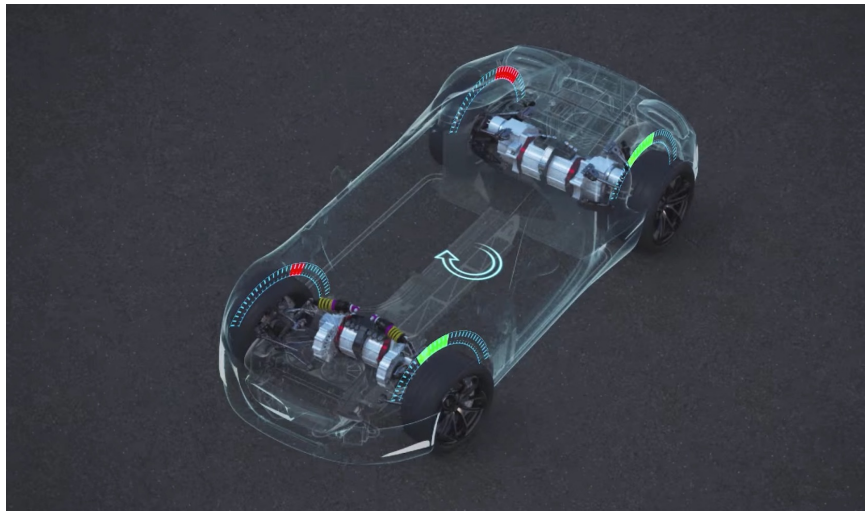


**Figure 2.3:** An example of EV using one motor on each wheel - Rimac Concept One; picture adopted from [4]

The next step from the previously mentioned series propulsion is to replace the ICE engine as a power source with the battery completely. The realization stays the same, either each powered wheel can be powered independently with its own motor or there is one (two) motor powering the whole axle.

In case the motor powers more than one wheel, it is missing the clutch and the generated torque is distributed by the final drive unit to the wheels. All the limitations on control remain, the only change is that the motor response is faster.

The EV in focus of this thesis has both rear wheels<sup>1</sup> powered by its own motor. The setup with one motor on every wheel, which can be seen in figure 2.3, has several advantages:

- Since each wheel has its own motor, the motors can be in general 'smaller' and less powerful than the motor that powers the whole vehicle. This can also lead to a better performance as the total torque might be larger than a one larger motor would generate.
- No need to install a final drive unit. If the wheel on each side has its own motor, the torque distribution does not require any additional mechanical parts as it is managed purely by the control unit. That can also lead to a reduction of mass of the vehicle.

<sup>1</sup>The assignment was prepared for a rear drive vehicle. The model and the final vehicle the thesis operates with and was supposed to be tested with, the student e-formula on the CTU, has all wheel drive with four electric motors.



The concept of having one motor per wheel also gives more possibilities in terms of control as it is described in the next chapter. The real vehicle chassis with two motors on one axle can be seen in figure 2.4, which shows the realisation as done in Tesla Model S. Though the EVs adopting this setup are still rather concept cars, their development receives a lot of attention.

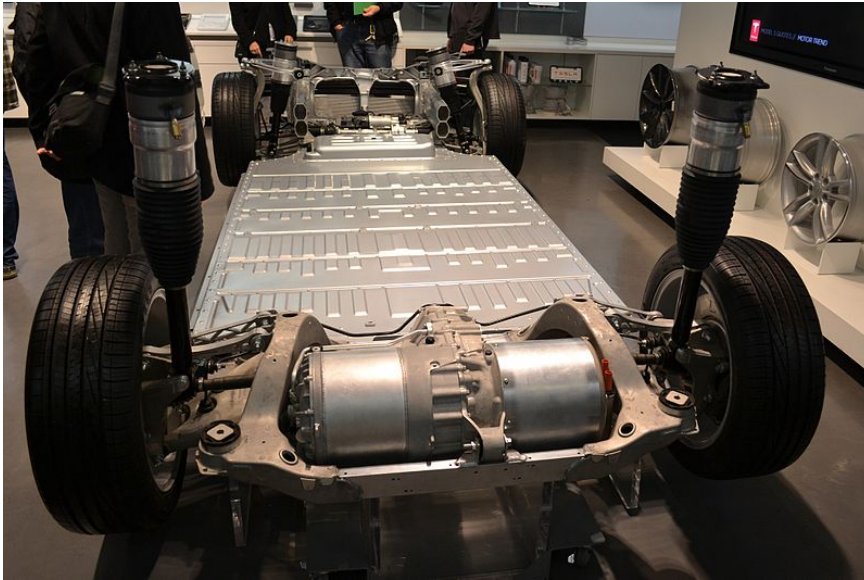


**Figure 2.4:** A concept chassis for an EV with one motor per wheel, solution used in Tesla Model S; picture adopted from [6]

## 2.2 Tractive force

Common to all described vehicles, the engine/motor generates mechanical torque which is transmitted via drivetrain to wheels, where it is transformed into a tractive force. Due to the tractive force, the vehicle is able to accelerate. To accelerate in straight direction, the forces generated by all wheels shall be ideally equal or the difference shall be negligibly small. If a difference appears and one side is generating more force than the other, a yaw torque is generated.

The tractive force is dependant on several different factors. It depends mainly on:

- the tires and their parameters, but also on their condition and structure;
- road condition and surface;

## 2. *Electric and internal combustion engine vehicle*

---

- relative motion between the wheel and the surface;
- normal loading.

The loss of tractive force is not very common but it can result in the vehicle becoming unstable and/or crashing in the worst case. The conditions are usually close to extremal situations, for example accelerating from standstill with maximum possible power and turning (can result into the vehicle to start skidding), accelerating on an icy road (the vehicle does not accelerate at all) etc. To avoid these situations, the traction control system is required.

## Chapter 3

### Vehicle control systems

There are many systems that ensure vehicle's and passengers' safety and comfort. Some of them watch over the vehicle's surroundings and react with only visual or audible warnings, some might override the driver's action, some only partially or in a way that driver stays in full control of the vehicle and other systems operate on a single component on a lower level.

The following chapter provides introduction to the traction control system and torque vectoring with the state of the art.

#### 3.1 A general overview

Current vehicles use a number of mechanical and electrical systems. They can be divided into several groups based on their purpose and the type of integration.

The oldest systems being in use are the passive systems and systems that secure the vehicle to be working properly. The most basic systems in this area are those ensuring the engine to work (fuel system, exhaust) and driveability of the vehicle (steering, brakes). These systems began as purely mechanical solutions.

Still as mostly mechanical solutions the passive safety systems emerged later. The passive safety focuses on preventing or minimizing possible injuries to the passengers and/or to the environment around. In addition to the passive safety systems related to so called interior safety according to [3], which are seatbelts and airbags (using electrical accelerometers) as the generally known solutions, the design of the vehicle itself contributes to safety of both the

interior and exterior. For the interior safety the design can contribute with fire protection. The exterior safety is determined by design in terms of the shape of the vehicle and the deformation behaviour in case of an accident.

On top of the mechanical part, active systems were developed to enhance the vehicle controllability and safety. These systems actively interfere with driver's immediate action, for example the *Antilock Braking System* (ABS) and *Traction Control System* (TCS). While the TCS is limiting the torque generation from the engine to prevent excessive slip ratios on the tire (further description of the system can in the upcoming section 3.2), the ABS lowers the brake pressure so that the wheels do not lock.

Another example of more advanced system is the *Electronic Stability Program*, known to drivers as ESP. The ESP can stabilize the vehicle in (mostly) sudden maneuvers in higher speeds. An example can be seen in figure 3.1 where a car is performing a double lane change maneuver. The ESP is able to detect the extreme situation and based on the driver's input (steering wheel angle) it can add brake pressure on certain wheel(s) to achieve a stable maneuver without the vehicle skidding. A more advanced solution includes the TV feature which can redistribute the unused torque from the inner wheel and apply it on the outer wheel.

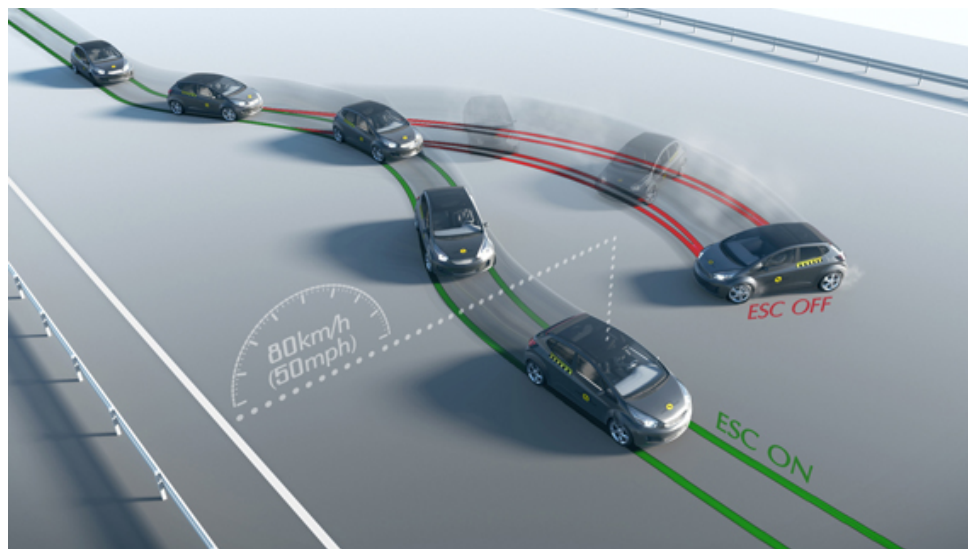


**Figure 3.1:** An example of the ESP system in use; picture adopted from [17]

The last, more complex systems are driver assistants. The main difference between an assistant and a safety system is that the assistant's action cannot fully override the driver. For example a lane assist, which helps the driver to keep inside his lane, moves the steering wheel in case the vehicle drives too close to the line. The driver can however override this - if there is a line crossing on a motorway, for example when there is a construction site, crossing a white line to follow the detour often triggers the line assist action. Other than that, there is the (adaptive) cruise control keeping the speed (and distance) from the previous vehicle, parking assistants giving audible

signals when approaching a solid obstacle, emergency braking system etc. To summarize the assistants, they help the vehicle safety, but mostly they enhance the driver's comfort experience while driving.

Today, the systems used in a vehicle are usually decoupled - they are installed in a car separately from each other and usually there is no necessary cooperation between them. The reason is that some of the functions are optional and the customer decides whether they shall be installed or not. Decoupling the systems might result in a less effective solution as in one certain moment the TCS (ESP) and torque vecoring might aim for a same solution while the TCS limits by default the possible action leaving less operational space for any other system. This thesis considers these functionalities (TCS and TV) as fully integrated in one system.

## 3.2 Traction control system

### 3.2.1 Functionality

As it was mentioned in the introductory section of this chapter, the TCS is a part of active vehicle safety systems, more specifically the ESP.

The main purpose of the TCS is to limit the rotation rate of a wheel to prevent excessive slip of the wheel which leads to a loss of the traction (and potentially also loss of stability) and ineffective power transmission. The figure 3.2 shows the transmitted force with changes of the vertical load on a wheel. The loss of tractive force defined by the excessive wheel slip ratio, as

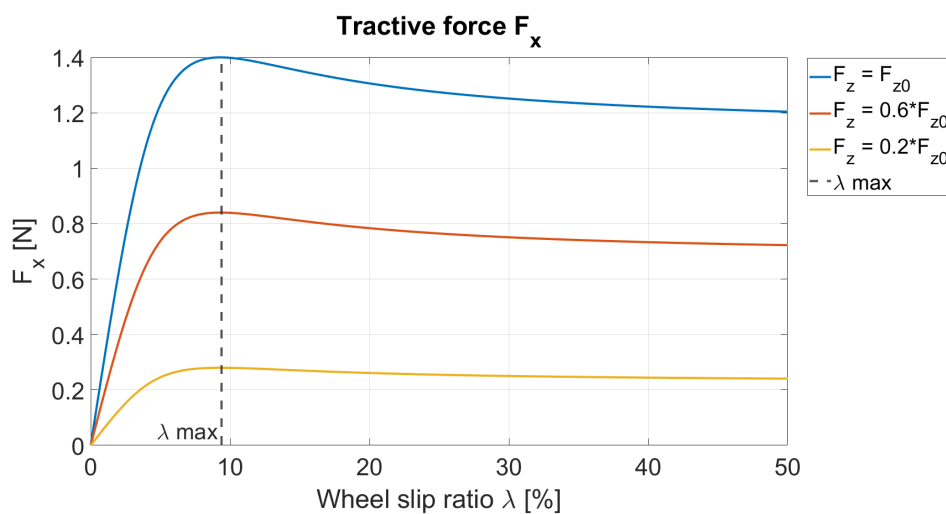


Figure 3.2: Tractive force based on Pacejka's magic formula

shown in figure 3.2, may be caused mainly by:

- low  $\mu$ ;
- low vertical load on a wheel.

While the wheel slip can be controlled, the vertical load and the road surface are mostly unknown and the TCS shall react in minimum time first to ensure the vehicle stability and, if possible, acceleration.

Additionally, the ESP stabilizes the vehicle in cornering maneuvers by both limiting the wheel slip and applying pressure on brakes. While performing a maneuver on the verge of vehicle stability (e.g. double lane change in a high speed) the ESP system prevents the vehicle from skidding and potentially endangering its passengers and surroundings. Another use case requiring a TCS is acceleration when crossing another lane or when overtaking.

### ■ 3.2.2 Algorithms

The implementation of the TCS system usually differs as each manufacturer might choose a different approach. However, according to the handbook [3], the TCS consists of three main parts:

- a vehicle state observer;
- a control unit evaluating the driver's command;
- a final controller.

Generally, the TCSs presented in the literature mostly deal with estimating road conditions based on models and comparison between the model output and measurement. As for the ICE, the control described in [3] combines all possible elements to compensate for slipping: lowering the torque from engine, applying pressure on brakes and eventually locking the differential on the slipping wheel.

The EVs offer other possibilities for the estimations of the road conditions and TCS itself. As presented in [8], the road type is estimated from its acoustic properties. The TCS then uses this estimation to calculate the maximum transmissible torque or passes this information to the slip ratio controller which aims at achieving the optimal value of  $\lambda$ . This algorithm is

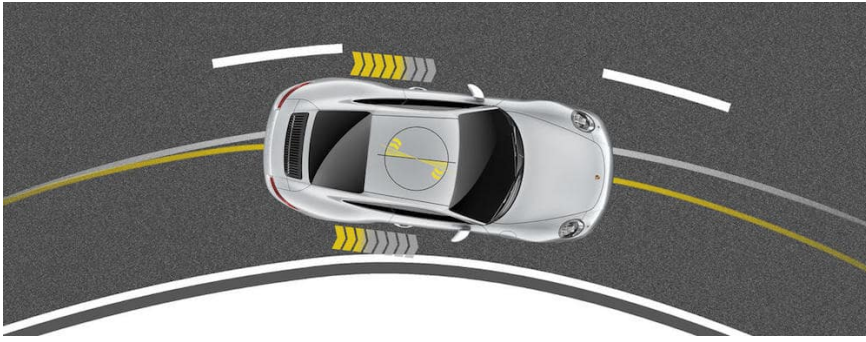


**Figure 3.3:** An example of TV, cornering maneuver; picture adopted from [7]

usable only in EVs as their motors produce less noise and vibrations than an ICE <sup>1</sup>. Similar control is presented in [9] just with the estimation based on a nonlinear observer. Another possible control is via model predictive control (MPC) as presented in [10] with constraints put on both vehicle states and inputs.

With the EV, the TCS has the ability to control the wheels directly and in addition the response of the motor is faster compared to an ICE vehicle. However with only one motor the control is still limited as the motor powers both wheels and the overall performance might drop. With one motor for each powered wheel, the slip ratio can be controlled directly on the slipping wheel without limiting other wheel and without any need for advanced and complex differentials.

### ■ 3.3 Torque vectoring

Apart from the TCS, TV is not a safety element but rather a yaw-control part. TV makes it possible to distribute torque to powered wheels inequally in order to improve the vehicle performance or compensate for sudden disturbances coming from the road or steering, not to achieve better traction. Other than that it helps in cornering maneuvers where it improves the vehicle's behavior to perform as a neutral vehicle in terms of steering. An example of TV functionality can be seen in figure 3.3, where the vehicle is performing a cornering maneuver. The yellow arrows mark the torques on each side of the vehicle. The left wheel on the outer side is powered by higher torque and produces the yaw torque.

<sup>1</sup>According to [13], the noise level between an EV and an ICE vehicle equalizes at about 30 km/h. The biggest difference in noise levels is about 20dB when both vehicles were stationary.

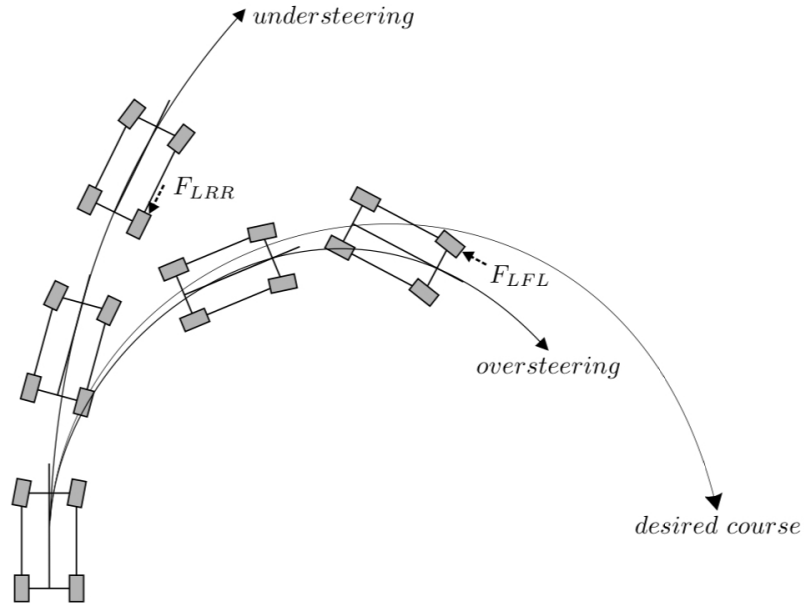


**Figure 3.4:** An example of behavior of an understeering, oversteering and neutral (pictured as *desired course*) vehicle adopted from [2]. The figure shows a possible solution adopted from the ESP when brake pressure is applied to slow the inner or outer wheel to achieve neutral steer.

### 3.3.1 Understeering, oversteering and a neutral vehicle

To understand the advantage of TV, it is helpful to remind the definition of neutral steering, oversteering and understeering and what their effects on vehicle might be during the cornering maneuvers.

Whether the vehicle is understeering, oversteering or neutral is determined mostly by its construction design. This characteristic has an impact on the vehicle performance during cornering maneuvers as it can be seen in figure 3.4. First, the steady-state steering angle  $\delta$  is defined (and adopted from [11]) as

$$\delta = \frac{L}{R} + K_V a_y, \quad (3.1)$$

where  $L$  is the vehicle wheel base,  $R$  is the radius of turn and  $a_y$  is centrifugal acceleration defined as

$$a_y = \frac{V_x^2}{R}, \quad (3.2)$$

with  $V_x$  being the vehicle velocity along its x-axis. The coefficient  $K_V$ , called the understeering coefficient, is then used to define the characteristic of the vehicle as seen in table 3.1. The figure 3.5 then in addition shows the dependency of  $\delta$  on  $V_x$ . It is apparent that with the growing longitudinal velocity the effect of non-neutral steering is not negligible and might result in loss of control over the vehicle.



| $K_V$     | Property      | Wheel slip angles     |
|-----------|---------------|-----------------------|
| $K_V = 0$ | Neutral steer | $\alpha_f = \alpha_r$ |
| $K_V > 0$ | Understeer    | $\alpha_f > \alpha_r$ |
| $K_V < 0$ | Oversteer     | $\alpha_f < \alpha_r$ |

**Table 3.1:** Values of understeering coefficient and how it indicates the slip angles relation for front ( $\alpha_f$ ) and rear ( $\alpha_r$ ) wheel [11]

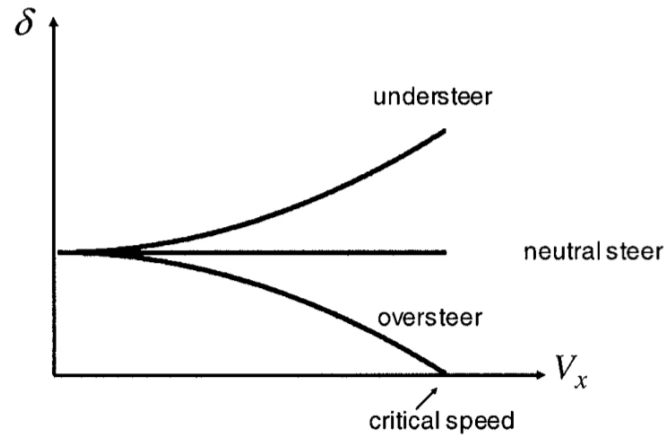


**Figure 3.5:** Dependency of the steering angle  $\delta$  on longitudinal velocity  $V_x$  for all types of steering; adopted from [11]

### ■ 3.3.2 Current torque vectoring systems

The TV feature implementation differs depending on the vehicle technical setup. The first option, for both ICE vehicles and EVs with one motor for multiple wheels, is to use a torque vectoring differential as described in [3] and [12]. For any other differential the TV feature cannot be used. Second option is applicable for EVs with one motor per powered wheel where the different torques are easy to be set.



## Chapter 4

### Mathematical models

For the development of the control, a corresponding framework has to be chosen and prepared. Within the framework there are three models defined: a design model, which is a linearized model used entirely for the development and early testing, a nonlinear high fidelity model for testing the original control and a verification model for evaluating the control over predefined maneuvers and scenarios. The verification model is supposed to be the most detailed and complex.

Both design and high fidelity model were implemented and tested with Matlab and Simulink (version R2020a), the verification was carried out in IPG Carmaker connected to Simulink.

#### 4.1 Mathematical model of the vehicle

There are several possibilities how to model a car: a simplified single-track model considering all four wheels with the vehicle track to be zero; or a full twin track model with all 4 wheels. In between these two models it is possible to merge them together to obtain a three-wheeled model with two wheels in rear and one in front (depending on the setup of the vehicle and the powered wheels). As the vehicle in focus of the thesis is supposed to be using TV and has electric motors installed on both rear wheels, the four wheel model was chosen as the most suitable. Also this approach makes any possible improvements (e.g. adaptation to all wheel drive) possible within a short period of time <sup>1</sup>.

---

<sup>1</sup>The control was tested on a model of CTU e-formula capable of all wheel drive. In case

It is important to define the vehicle coordinates in order to describe the movement in all directions. The longitudinal movement is defined along the x axis, the lateral movement along the y axis and the last, z axis, is vertical according to the right hand coordinate system. The origin of the coordinate system is put in the vehicle's center of gravity (CoG). The same principle applies also to the wheel which has its own coordinate system as shown in figure 4.1.

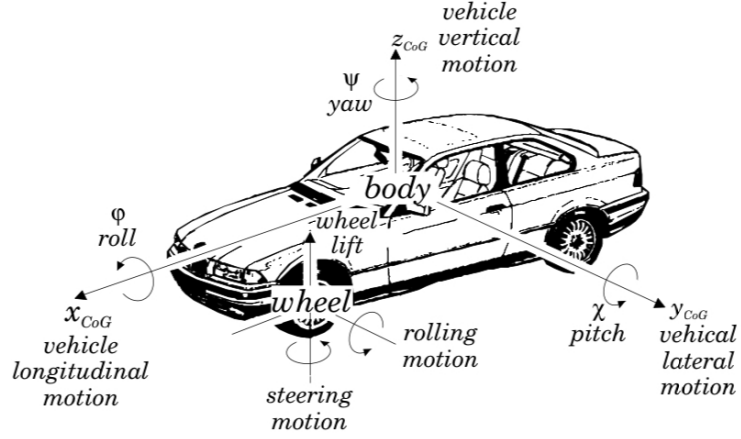


**Figure 4.1:** Two principle vehicle coordinate system; picture adopted from [2]

#### 4.1.1 Dual track vehicle model

The high fidelity dual track model was adopted from [14] and [15]. The model describes only the planar motion - longitudinal, lateral and yaw motion (around its z axis). Pitch movement, rolling and lifting is neglected.

The vehicle motion in the longitudinal direction is described by equation

$$-mv(\dot{\beta} + \dot{\psi})\sin(\beta) + m\dot{v}\cos(\beta) = F_x, \quad (4.1)$$

where  $m$  is the vehicle mass,  $v$  is the vehicle velocity,  $\beta$  is the vehicle side slip angle and  $\dot{\psi}$  is the vehicle yaw rate. The lateral movement is described as

$$-mv(\dot{\beta} + \dot{\psi})\cos(\beta) + m\dot{v}\sin(\beta) = F_y \quad (4.2)$$

and for the yaw motion applies

$$I_z \ddot{\psi} = M_z, \quad (4.3)$$

the control would be tested on a real vehicle, a question was raised whether the control can be modified to an all wheel drive setup.

where  $I_z$  is the moment of inertia of the vehicle. These can be rewritten in a matrix form as

$$\begin{pmatrix} mv(\dot{\beta} + \dot{\psi}) \\ m\dot{v} \\ I_z\ddot{\psi} \end{pmatrix} = \begin{pmatrix} -\sin(\beta) & \cos(\beta) & 0 \\ \cos(\beta) & \sin(\beta) & 0 \\ 0 & 0 & 1 \end{pmatrix} \begin{pmatrix} F_x \\ F_y \\ M_z \end{pmatrix}. \quad (4.4)$$

Since there are four wheels in the model, it is important to take into account all contributions from these wheels as, based on the steering angle of the front (and possibly rear) wheels, all the forces may differ in general. It is then possible to write down

$$\begin{pmatrix} F_x \\ F_y \\ M_z \end{pmatrix} = \begin{pmatrix} c(\delta) & c(\delta) & 1 & 1 & -s(\delta) & -s(\delta) & 0 & 0 \\ s(\delta) & s(\delta) & 0 & 0 & c(\delta) & c(\delta) & 1 & 1 \\ x_1 & x_1 & x_4 & -x_4 & x_2 & x_3 & x_5 & x_5 \end{pmatrix} \begin{pmatrix} F_{xfr} \\ F_{xfl} \\ F_{xrr} \\ F_{xrl} \\ F_{yfr} \\ F_{yfl} \\ F_{yrr} \\ F_{yrl} \end{pmatrix}, \quad (4.5)$$

where

$$c(\delta) = \cos(\delta), \quad (4.6)$$

$$s(\delta) = \sin(\delta), \quad (4.7)$$

$$x_1 = p_f \sin(\delta + \phi_f), \quad (4.8)$$

$$x_2 = p_f \sin(\delta + \phi_f), \quad (4.9)$$

$$x_3 = p_f \cos(\delta - \phi_f), \quad (4.10)$$

$$x_4 = p_r \sin(\phi_r), \quad (4.11)$$

$$x_5 = -p_r \cos(\phi_r). \quad (4.12)$$

The variable  $\delta$  represents the steering wheel while coefficients  $p_r$ ,  $p_l$ ,  $\phi_r$  and  $\phi_f$  describe the position of each wheel in the coordinate system of the vehicle as shown in the figure 4.2. The steering angle  $\delta$  is the input to the system.

With respect to previous equations, the final state equations are expressed as

$$\dot{\beta} = -\dot{\psi} + \frac{1}{mv} [\cos(\beta)F_y - \sin(\beta)F_x], \quad (4.13)$$

$$\ddot{\psi} = \frac{1}{I_z} M_z, \quad (4.14)$$

$$|\dot{\vec{v}}| = \frac{1}{m} [\sin(\beta)F_y - \cos(\beta)F_x], \quad (4.15)$$

where  $m$  is the vehicle mass,  $|\vec{v}|$  is the vehicle speed,  $I_z$  is the moment of inertia of the vehicle for yaw motion,  $\beta$  is the side slip angle and  $F_x$  and  $F_y$  are the forces along the respective axes of the CoG coordinate system. The wheel model will be described further in the next section.

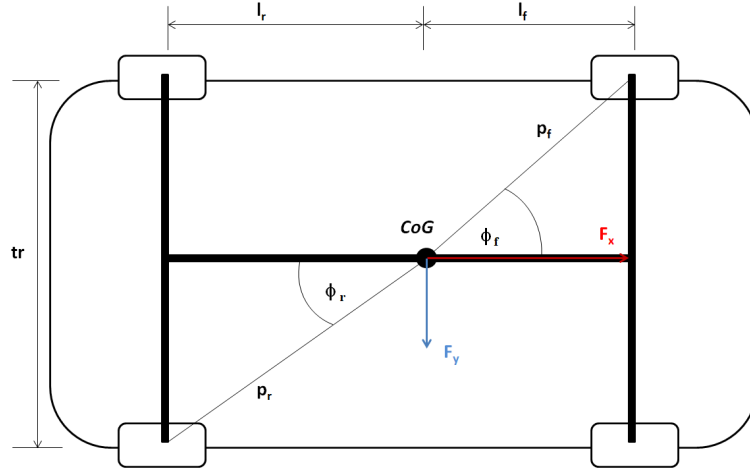


**Figure 4.2:** A simple vehicle scheme showing coefficients associated to wheels positions

#### 4.1.2 Wheel model

The implemented twin track model supposes that each wheel is powered by an individual electric motor. Generally, the equation for each wheel rotation rate can be written as

$$\dot{\omega} = \frac{\tau - RF_x - k_d v_x}{I}, \quad (4.16)$$

where  $\tau$  is the torque generated by the corresponding motor,  $R$  is the wheel radius,  $k_d$  is the drag coefficient,  $I$  is the moment of inertia of the wheel and the powertrain and  $v_x$ ,  $F_x$  are the velocity and the force along the x axes in the wheel coordinate system, respectively. The model in this form neglects the braking torque and works only with the torques generated by the motors. Hence four additional inputs on top of the steering angle are introduced to the model. It is also important to notice that the motors are connected to a fixed transmission first. This is already included in the model therefore the torque  $\tau$  in the equation 4.16 is the torque generated at the output of the transmission.

As the vehicle in focus of the thesis is a rear drive only, the torques on the front wheels are considered to be zero. The full model however gives the option to incorporate the all wheel drive with minimum modifications if needed.

It is also important to notice that each wheel may have a velocity different from the velocity of the vehicle and from the other wheels. For the front wheels' velocity in x axis in the CoG coordinate system equation

$$v_{xfr,l} = v \cos(\beta - \delta) + p_f \dot{\psi} \sin(\delta \pm \phi_f), \quad (4.17)$$

applies and for the rear wheels equation

$$v_{xrr,l} = v \cos(\beta) + p_r \dot{\psi} \sin(\pm \phi_r) \quad (4.18)$$

| Surface       | $\mu$ [-] |
|---------------|-----------|
| Asphalt, dry  | 1.28      |
| Concrete, dry | 1.20      |
| Asphalt, wet  | 0.86      |
| Snow          | 0.19      |
| Ice           | 0.05      |

**Table 4.1:** Values of  $\mu$  for various road surfaces; based on Buckhardt as stated in [2]

applies, where  $v$  is the vehicle's velocity,  $\dot{\psi}$  is the yaw rate,  $\delta$  is the steering angle and  $\phi_{f,r}$ ,  $p_{f,r}$  are constant values of angles from the vehicle's x axis defined by the CoG and the distance from the CoG.

The torque delivered to wheel is then trasformed into tractive force, which is usually a function of wheels' and vehicle's velocity. There are several ways how to define this force. The thesis operates with the force generated by tires as defined by Hans Pacejka in the general (and simplified) form of equation 4.19 introduced in [1] as the Pacejka's magic formula.

$$F(x) = D \sin [C \arctan \{Bx - E(Bx - \arctan Bx)\}], \quad (4.19)$$

where the  $F$  is the force generated by the wheel and coefficients  $B$ ,  $C$ ,  $D$ ,  $E$  are a set of parameters defining properties of the tire. Furthermore, the coefficient  $D$  stands for

$$D = \mu F_z D_0, \quad (4.20)$$

where  $D_0$  is the parameter of the tire, but without the influence of the vertical force  $F_z$  and the road friction coefficient  $\mu$ . This introduces the road friction coefficient  $\mu$  and vertical force  $F_z$  applied on the wheel to the original equation 4.19. While  $\mu$  is dependant on the road surface (examples for various surfaces can be seen in table 4.1), the  $F_z$  might vary based on driving conditions and situations. The equation then changes to the form shown in equation 4.21

$$F(x, F_z, \mu) = \mu F_z D_0 \sin [C \arctan \{Bx - E(Bx - \arctan Bx)\}] \quad (4.21)$$

The force as defined in equation 4.21 applies to forces in both longitudinal and lateral dynamics using different sets of parameters and the variable  $x$ . For the force in longitudinal motion the variable  $x$  is substituted with the wheel slip ratio  $\lambda$  defined for acceleration as

$$\lambda = \frac{\omega r - v_x}{v_x}, \quad (4.22)$$

for decelariton the  $\lambda$  becomes

$$\lambda = \frac{\omega r - v_x}{\omega r}, \quad (4.23)$$

where  $r$  is the wheel radius,  $\omega$  is the wheel rotation rate and  $v_x$  is the vehicle velocity along the x axis of the CoG coordinate system. and for the lateral motion the force it is substituted with the wheel slip angle  $\alpha$  defined as

$$\alpha = -\arctan\left(\frac{v_x}{v_y}\right). \quad (4.24)$$

The forces are then defined as

$$F_x = f(\lambda, F_z, \mu), \quad (4.25)$$

$$F_y = f(\alpha, F_z, \mu). \quad (4.26)$$

The total force is bound by so called friction ellipse, sometimes can be found as the Kamm's circle, which can be seen in figure 4.3.

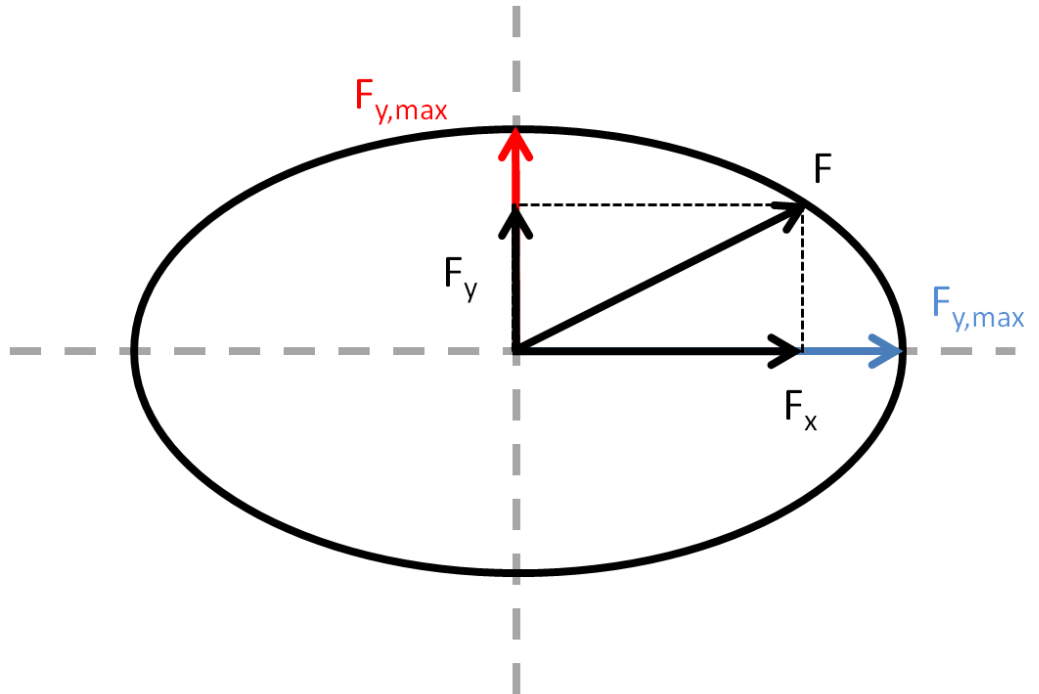


**Figure 4.3:** An example of Kamm's (friction) circle

The loss of tractive force can affect the vehicle in several ways. An example can be given with the help of figure 4.4. The figure shows an example of a split  $\mu$  road test where the vehicle's right side is driving on ice. In case that the TCS is not installed, the longitudinal slip on powered wheel(s) will grow which leads to the loss of traction. In addition, the left wheel stays on a regular road (or higher  $\mu$  surface) and the tractive force remains higher than on the right side resulting into yaw movement. Similar situation might happen if the vehicle drives off the road with one side, for example when avoiding another vehicle in the opposite direction or possible bump on the road.

The tractive force might be also lowered while accelerating from standstill





**Figure 4.4:** An example of split  $\mu$  road on a testing site; picture taken from [16]

or when overtaking - this can happen again on a low  $\mu$  surface or when the requested acceleration is too high and the engine/motor is powerful enough to make the wheels slip.

## 4.2 Design model and verification

For the purpose of the development and early-testing of the control desing, the high fidelity model had to be linearized. For this purpose the linearization tool, developed and provided by Petr Turnovec and David Vošahlík (the tool can be found on the enclosed CD), was used. The deviation model represented by the following equations was chosen and implemented:

$$\Delta\dot{x}(t) = A\Delta x(t) + B\Delta u(t), \quad (4.27)$$

$$\Delta x(t) = x(t) - x_0, \quad (4.28)$$

$$\Delta u(t) = u(t) - u_0, \quad (4.29)$$

with  $A$ ,  $B$  being the state matrices and  $[x_0, u_0]$  being the operation point.

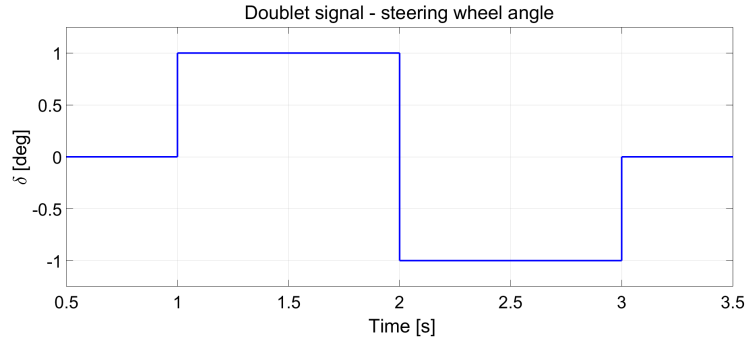


**Figure 4.5:** Doublet source signal

The model can be then rewritten as

$$\Delta \begin{pmatrix} \dot{\beta} \\ \ddot{\psi} \\ \dot{v} \\ \dot{\omega}_{fr} \\ \dot{\omega}_{fl} \\ \dot{\omega}_{rr} \\ \dot{\omega}_{rl} \end{pmatrix} = A \Delta \begin{pmatrix} \beta \\ \dot{\psi} \\ v \\ \omega_{fr} \\ \omega_{fl} \\ \omega_{rr} \\ \omega_{rl} \end{pmatrix} + B \Delta \begin{pmatrix} \delta \\ \tau_{rr} \\ \tau_{rl} \end{pmatrix}. \quad (4.30)$$

It is necessary to validate the linearized model against the original nonlinear model. The results proved the linearized model to be valid for further development. An example response to a doublet signal (shown in figure 4.5) as one of several preformed tests is displayed in figure 4.6.

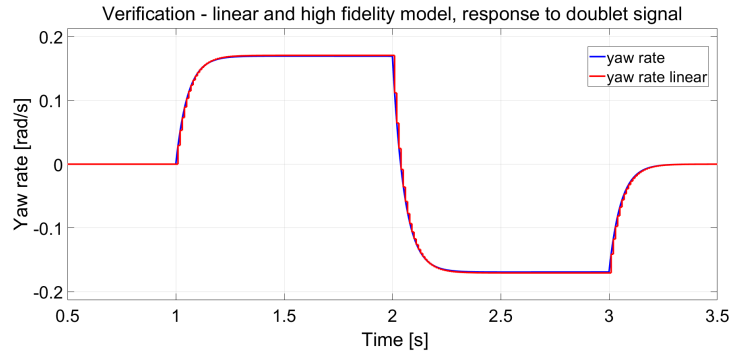


**Figure 4.6:** Verification of the linear model, response to doublet signal on the steering wheel

The last tool used for verification was the IPG Carmaker. The simulation carried out in this environment is more complex as it takes into account also the motions neglected in the design model. This tests how the control algorithm might behave in the real vehicle as the conditions also change based on (mostly) pitch and roll motion. Also it is capable to test how the vehicle behaves in case it was driven by a driver.

## 4.3 External conditions model

Since the thesis is focused on the TCS, it is necessary to be able to modify the external conditions, which is for the purpose of the thesis limited to the road surface. Any changes in the characteristics of the road are reflected with the properties of  $\mu$  parameter as shown in equation 4.21.

The change of the  $\mu$  value is, in case of the linear model, done with loading a different set of system matrices. In the high fidelity model in Simulink the change is done by parsing the current value of  $\mu$  to the corresponding wheel subsystem that calculates the forces applied to the vehicle. Both these models allow easy changes in the environment which make it possible to test the control performance even on uneven road surface. The values of  $\mu$  were chosen from the interval

$$\mu \in \langle 0.2, 1 \rangle, \quad (4.31)$$

where the lowest value, according to the table 4.1, corresponds to snow on the road.





## Chapter 5

### Control design

The third chapter of this thesis provided a brief introduction to the functionality of the TC and TV systems and the current state of the art. Most of the described systems however operate with the fact that both these systems are separated from each other as they are typically included based on the customer specific request and not necessarily both at the same time. As a consequence, these systems are independently trying to find an optimal solution while the overall performance might be negatively impacted.

The control proposed in this thesis aims at combining these systems together into one controller which shall optimize the generated torques.

This chapter summarizes the requirements on the controller (and vehicle). It also describes possible scenarios where the control should be applied and tested and at last the implementation is further described.



#### 5.1 Performance requirements

It is important to define the requirements in order to develop the control algorithm. Some of the requirements set very specific constraints on the final controller while other leave some space in implementation (and possible future improvements). The requirements can be divided into two groups:

- requirements towards the overall vehicle performance;
- requirements on the control from the motor point of view.

First, the vehicle performance requirements are discussed, then the requirements towards the control follow.

### ■ 5.1.1 Vehicle performance requirements

This set of requirements mostly describes the general behavior of the vehicle. It serves as an outline for the controller and for its interface. The requirements are listed below with a short comment on their necessity.

#### ■ The vehicle shall never exceed referenced velocity.

The section 4.1.2 describes the model and its states. There are several possible ways how to approach the acceleration pedal signal. For the purpose of this thesis, the signal from the pedal is considered to be setting the velocity reference as an input from the driver. This requirement is crucial as the TCS directly influences the motors.

As for the TV, since it is able to distribute the torques inequally on both wheels, the velocity reference in cornering maneuvers can be exceeded. The control might lead to a solution which would increase one or both torques. That might result in higher velocity than demanded while the correct approach would be to limit the other torque.

With this requirement, the first two necessary inputs to the controller are defined: the velocity reference and current vehicle velocity.

#### ■ The controller shall detect excessive wheel slip ratio. If the wheel slip ratio exceeds a given threshold, the controller shall lower it.

This requirement defines the basic concept of the TCS. The wheel slip ratio may grow beyond the optimal value (which is about 10% specified in section 2.2). It can happen when the demanded acceleration requires torque change resulting in the wheel slipping, when the vehicle drives on a low  $\mu$  surface or if the vertical load on the wheel is lowered.

Since the force generated by the tire is defined by the wheel slip ratio  $\lambda$ , the rear wheels rotation rates become another required input to the controller.

■ **The controller shall stabilize the vehicle.**

If we consider a use case when the vehicle drives with its one side on a low  $\mu$  surface (for example in winter the outer side of the road might be covered with ice), the force generated by this tire decreases and the vehicle's yaw rate  $\dot{\psi}$  becomes non-zero. The controller shall redistribute the torques on each motor so that any disturbance is eliminated and yaw rate is driven to the reference value.

Since the requirement describes the TV functionality (ability to inequally redistribute traction torques), it is necessary to know the current steering angle. Therefore the controller shall follow a referenced yaw rate  $\dot{\psi}_{ref}$  defined by the steering angle  $\delta$ .

■ **The torques on the motors shall be always positive.**

As it was outlined in the section 2.1, the powertrain of an EV is quite simple and, consequently, a negative torque request is possible in principle. However processing a negative torque request from the controller might result into more aggressive yaw rate addition from the TV and, combined with further requirements, might lead to drop in overall performance.

In case of braking, the preferred option is to use brakes with lowering the motors' generated torques to zero and not setting the torque to negative values.

■ **The torques shall not exceed the motor maximum.**

The motors used on the vehicle have a maximum torque they are able to generate. This value shall not be exceeded and the controller shall have this information available to ensure optimal performance.

■ **The controller shall contain a rate limiter related to the controller's output.**

The general advantage of an EV is that the electric motor's response is faster than a regular ICE's. However the response is not infinitely fast and

sudden changes in applied torques are undesirable.

Not only the rate limiter prevents the sudden changes, it can be also considered as a performance requirement as large sudden changes might result in jerks in vehicle motion. Since it is not known whether (and how) there is a rate limiter for the requests already implemented, the controller shall contain its own.

■ **The difference between left and right motor torque shall be limited.**

Since the TV feature is also implemented, the controller is able to distribute the torques inequally thus generate vehicle yaw momentum. The momentum grows with the difference between the wheel rotation rates and the higher the speed, the lower the difference. In some cases the TV feature is even turned off. As a result, the difference between wheel torques should be limited, ideally based on speed, less ideally with a constant value suitable for most of the driving situations.

■ **The control unit shall operate on a 100Hz frequency.**

The control unit shall be able to produce a solution in a given time window to guarantee an immediate response to the situation or the request. In this case, the unit is given a 10ms long window for its computations.

■ **5.1.2 Scenarios**

To test the controller performance, several driving situations requiring the TCS and/or the TV were chosen. The basic concept of the scenarios does not change but is performed repeatedly with different road conditions.

■ **Acceleration**

The most basic scenario for testing the implementation is the acceleration maneuver. The TCS shall be able to accelerate the vehicle on demand while preventing the excessive slip from both initial non-zero velocity and standstill.



It is possible to modify the scenario in several ways to test the whole controller. The defined scenarios are:

- A small disturbance on the steering wheel is introduced in order to check whether the TV part of the control is able to drive the yaw rate back to zero.
- A change in surface type while accelerating to test whether the TCS is able to lower the torque to prevent excessive slip ratios.
- The split  $\mu$  scenario. This variant combines action from both the TCS and the TV since the TCS shall lower the torque and the TV part shall bring the yaw rate to zero again while the vehicle shall continue accelerating. An example of a split  $\mu$  road is displayed in figure 4.4.
- Start with zero initial velocity. At standstill, the wheel slip ratio is not defined which might lead to a slow acceleration even in case of large velocity reference.

## ■ Cornering

Another typical maneuver for testing is the cornering. It tests the TV ability to follow the yaw rate reference set by the driver. The maneuver can now be performed while accelerating or at constant speed, on a regular road or on split/low  $\mu$ . The performance depends also on the situation, whether the maneuver is performed during a high or low speed, the steering wheel angle and so.

Other than the TV functionality, the TCS is tested as well. During acceleration while cornering the wheels shall obtain a different limit on their rotation rates and the slip ratio shall not exceed this limit.

An example of a cornering scenario can be seen in figure 5.1 where a vehicle accelerates from standstill into a turn. This situation might happen when another vehicle arrives from the opposite direction and the driver need to accelerate to avoid the possible accident. Another scenario, as shown in 5.2, might be a vehicle taking a long turn with constant velocity. The scenario is based on a real road which is relatively narrow. From time to time the vehicle in opposite direction drives too close to the center of the road forcing the driver in the vehicle pictured in the scenario to drive with one side of the vehicle out of the road. The different surfaces may be a cause for undesired yaw torque on the vehicle.

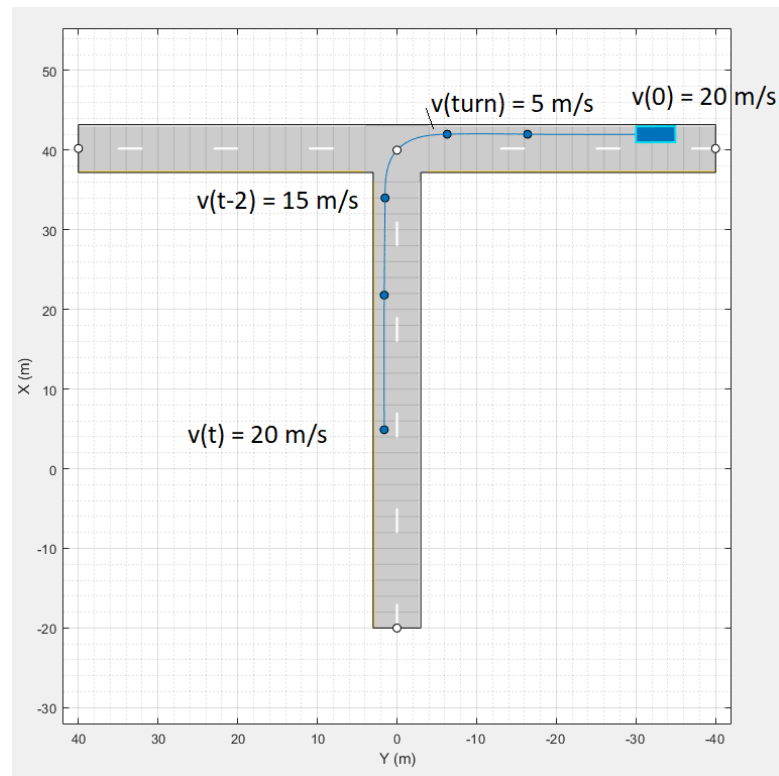


**Figure 5.1:** An example scenario for acceleration and cornering at the same time with velocity references along the trajectory. Designed in Matlab's Driving Scenario Designer.

## 5.2 Control development

With the requirements for the control defined, this section describes the development of the whole control system. The control presented here follows a feedback scheme described in figure 5.3 with input treated as reference coming from the driver. The control preconditions and possible simplifications are discussed in the next section.

This section also covers the signal processing from the IPG Carmaker, which was used as the testing tool for the control algorithm.

### 5.2.1 Assumptions, simplifications and limitations

There are several preconditions for the control to work properly. The preconditions are related to the driver's input and measurements.

The input consists of two signals, the steering angle and the acceleration

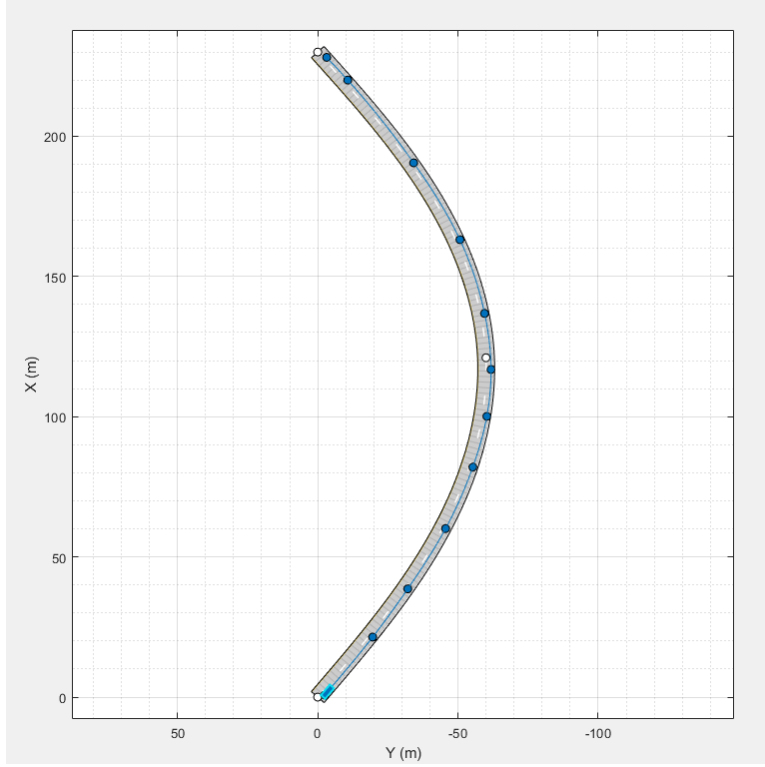


**Figure 5.2:** An example scenario of a long turn with possible split  $\mu$ . Designed in Matlab's Driving Scenario Designer.

pedal signal. The reference, based on these signals, then sets the target for the vehicle's velocity and its yaw rate. The yaw rate reference is recalculated from the steering angle as

$$\dot{\psi} = \frac{\tan(\delta)v}{l_r} \quad (5.1)$$

according to the kinematic model. This calculation applies to lower speeds, in higher speed it becomes inaccurate.

Another necessary input into the controller are the measurements of the vehicle states. In the design model, the states are taken directly from the nonlinear model. Otherwise the control has no other estimations, the states are considered to be measured. The only measurement which is considered to be unknown is the side slip angle  $\beta$ .

Among the measurements, the corrected values for wheel speed according to equations 4.17 and 4.18 are included as well. Whenever the controller operates with the wheel rotational rates limits, the calculation is further simplified and for the rear wheel velocities it becomes

$$v_{xrr,l} = v + k_r \dot{\psi}, \quad (5.2)$$

where

$$k_r = p_r \sin(\pm\phi_r). \quad (5.3)$$

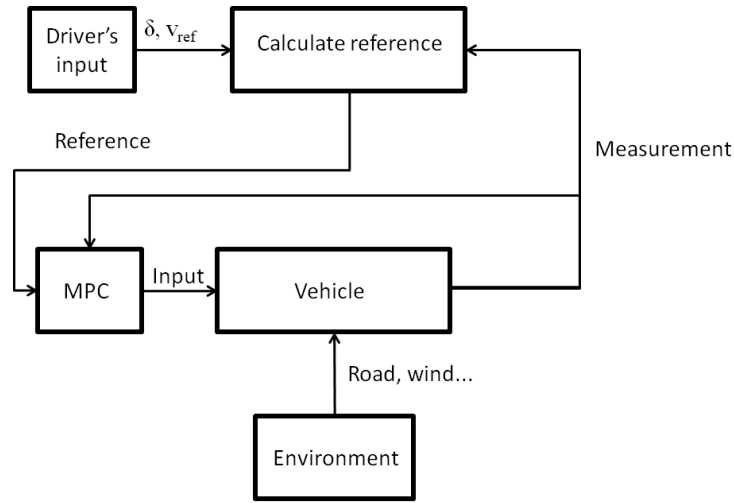


**Figure 5.3:** Control scheme

The value of  $\beta$  is considered to be negligibly small during the whole drivetime and therefore can be disregarded. The wheel velocity then becomes a function of the total vehicle speed and its yaw rate.

It is also important to note that the problem is formulated in delta-notation meaning that the calculations are incremental. It is then necessary to take into account the operational point together with its input in order to feed the controller the correct data. This applies both to the measurements and the reference.

The same approach is applied to the output as well, and when sending the torque command, the  $u_0$  value has to be added to the controller output. Also, the model works with the final value of torques which means that it already has incorporated the transmission on the motor. Therefore, before the output signal is sent, the torque has to be divided by the transmission ratio.

## ■ 5.2.2 Model Predictive Control

The model predictive control (MPC) is a type of feedback control algorithm. The 'model predictive' here indicates that the controller has information about the plant (in this case the vehicle), its states, inputs and outputs. According to [18], the controller seeks a feasible solution while minimizing a cost function and following a defined set of constraints. One of the most remarkable advantages of this control approach is that it can reflect changes in reference in the future time (to stick with the automotive theme, the example might be the autonomous vehicle approaching a sign with lower speed limit. The MPC

from certain point obtains the lower reference at the end of the reference vector and starts to brake slowly in advance). On the other hand, the solver searching for a solution requires computational power and time in order to find a feasible solution.

As already mentioned, the MPC consists of several parts. The first part is the objective function defined as

$$J(\vec{y}, \vec{u}, \vec{r}) = \sum_{k=0}^{N-1} |Q(\vec{y}_k - \vec{r}(t))|^2 + |R(\vec{u}_k - \vec{u}_r(t))|^2 \quad (5.4)$$

where  $\vec{y}_k$  is the vector of system outputs in the sample  $k$ ,  $\vec{r}(t)$  the vector of the given reference,  $\vec{u}_k$  is the vector of system inputs in the sample  $k$ ,  $\vec{u}_r(t)$  is the vector of the given reference, matrix  $Q$  is a positive semidefinite matrix of system states or output weights and  $R$  is a positive definite matrix of system input weights. The cost function can be defined in different ways based on the actual problem which the controller is supposed to solve.

Another part of the MPC is the model which can be either linear or nonlinear. It is usually sufficient to use a simplified linear model [18] rather than a very precise one as the computational time might increase. As the sum operation in equation 5.4 suggests, the model is usually time discrete. The model here follows the linear model given in equation 4.30.

The last input to the MPC are constraints on states, outputs and inputs. Usually there are an upper and lower bound specified so that

$$x_{lb} \leq x_k \leq x_{ub}, \quad (5.5)$$

$$y_{lb} \leq y_k \leq y_{ub}, \quad (5.6)$$

$$u_{lb} \leq u_k \leq u_{ub}, \quad (5.7)$$

which shall be complied with in every time sample  $k$ . If the conditions are met, the problem is then called feasible. If the solver cannot find a solution that satisfies the given constraints, the problem becomes infeasible. In case of infeasible problems the solver might return a value which is undesirable (e.g. motor producing its maximum possible torque might obtain command to immediately return to zero). The condition is usually not met with the outputs or states which the controller cannot get in the given bounds. This can happen with sudden changes coming from the unknown environment around the controlled plant or from modeling errors since the model is simplified and often linearized. To avoid infeasible problems, the constraints can be modified and they become so called soft constraints. These are given as

$$y_{lb} - \epsilon_{min} \leq y_k \leq y_{ub} + \epsilon_{max}, \quad (5.8)$$

where the  $\epsilon$  represents the 'panic' (or 'slack') variable. The existence of such variable has to be reflected in the objective function as well. The function is extended with a new part as

$$J(\vec{y}, \vec{u}, \vec{r}, \vec{\epsilon}) = J(\vec{y}, \vec{u}, \vec{r}) + \sum_{k=0}^{N-1} |Q_e(\epsilon_k)|^2, \quad (5.9)$$

where the  $Q_e$  is a new diagonal weight matrix for the panic variables. Usually for any non-zero weight  $q_e$  from weight matrix  $Q_e$  and for any weight  $q$  from weight matrix  $Q$  applies that

$$q_e \gg q. \quad (5.10)$$

The higher weight is required as the panic variable serves only for feasibility purposes. As a result, the solver shall act to lower the variable that gets out of bounds of the constraints due to the higher weight put on the 'panic' variable.

The last piece to be defined for the MPC is the prediction horizon and the sampling time  $T_s$ . Both the sampling time and the prediction horizon are connected with the use case. With the decreasing sampling time the disturbances caused by unknown parameters are rejected and the overall performance is better. On the other hand, the computational time increases with  $T_s$  becoming too small. Second part is the prediction horizon which, in the cost function 5.4, is represented by the  $N$ . Again, if the control horizon is too large, the computational time increases. Having the horizon too small can however produce an internally unstable controller. Both the sampling time and prediction horizon are parameters which are usually tuned during the development based on actual results. A more detailed guide on how to select the sampling time and the prediction horizon can be found on Matlab's website [19].

Based on the usage, the MPC is able to return the whole optimization input vector for each prediction step. Only the first value is then used for further control and the whole process repeats with newly obtained measurement.

## 5.3 Implementation

For the implementation, Matlab R2020a [20] was used as the language/environment. The prototype control was developed using the interface Yalmip [21] with Gurobi [22] as the solver. The main advantage of Yalmip is an intuitive formulation of the problem and the constraints. This makes the MPC debugging and tuning relatively simple. On the other hand, the control using Yalmip is not fast enough even with the fastest possible solution (creating an optimizer object) and it is not able to produce a binary code for actual use in a real vehicle.

The controller was initially given a time horizon of one second with the sampling time of 0.1s resulting into ten prediction steps of the MPC.

To begin with the constraints on the control, they follow the requirements stated in 5.1.1. The first constraint is applied on the first member of the vector of system inputs (MPC's outputs). The constraint is given as

$$abs(u_1 - u_0) \leq 0.01\tau_{max}, \quad (5.11)$$

where  $u_1$  is the first optimized input,  $u_0$  is the previous outputted torque command and  $\tau_{max}$  defines the maximum step between the torques. This condition can be understood as the rate limiter implementation that lets the controller change the torques from zero to maximum in time window of one second. Next, the other prediction steps were given a similar condition, only with the reflection of the different time step:

$$abs(u_{k+1} - u_k) \leq 0.1\tau_{max}, \quad (5.12)$$

The next constraint on the input sets the maximum and minimum allowed values of the torque. The condition is simply given as

$$0 \leq u_k \leq \tau_{max}. \quad (5.13)$$

The last constraint is related to the TV feature and is limiting the torque difference on both wheels as follows:

$$abs(u_l - u_r) \leq 0.1\tau_{max}, \quad (5.14)$$

which shows that the difference between wheels' torques cannot exceed 10% of the maximum torque.

The rest of the constraints is connected to the vehicle states. All these constraints are defined as soft constraints. For the velocity, the constraint is defined as

$$(v_{k+1} - v_{ref}) \leq v_s, \quad (5.15)$$

where  $v_{k+1}$  is the speed in following sample ( $v_k$  for  $k = 0$  is supposed to be the measured state) and the  $v_s$  is the panic variable. The referenced velocity shall be reached due to formulation of the control objective, however specifying that the control shall not exceed this value is rather a safety request. This constraint is formulated as a soft one because if the reference drops faster than the vehicle is able to slow down until next sample, the MPC would encounter an infeasible problem.

The remaining constraint is the constraint forming the TCS requiring that the rotation rates of the wheels shall not exceed a certain limit. The constraint is defined (for both wheels) as

$$(\omega_{k+1L,R} - \omega_{max,k+1,L,R}) \leq \omega_{sR,L}. \quad (5.16)$$

The maximum allowed value of the wheel slip ratio is set to 10% and from equation

$$\frac{r\omega_{max} - v}{v} = 0.1, \quad (5.17)$$

the wheel rotation rate limit is derived. Again, the constraint is given as a soft one since the wheel slip ratio may change rapidly with the change of surface type.

The next part of the MPC is the objective function with the defined weight matrices. The objective and the weight matrices are defined for every step and summed together following the algorithm 1. Extended to single states,

---

**Algorithm 1** Calculation of the objective function

---

**Require:**  $N > 1$ ;  $x_0$  known;  $x_{ref}$  known;  $u_0$  known**Ensure:**  $Q = \text{diag}([0 \ 2e+4 \ 1e+2 \ 0 \ 0 \ 0 \ 0])$ ; $R = \text{diag}([1e+2 \ 1e+2])$ ; $Q_s = \text{diag}([1e+7 \ 1e+7 \ 1e+7])$ ; $J \leftarrow 0$ **for**  $k = 1:N$  **do** $J \leftarrow J + (x(k) - x_{ref}(k))^* Q^* (x(k) - x_{ref}(k))$ ; $J \leftarrow J + (u(k) - u(k+1))^* R^* (u(k) - u(k+1))$ ; $J \leftarrow J + (x_s)^* Q_s^* (x_s)$ ;**end for**

---

---

**Algorithm 2** Calculation of the objective function, extended to single states

---

**Ensure:**  $J \leftarrow 0$ **for**  $k = 1:N$  **do** $J \leftarrow J + (\text{yawRate}(k) - \text{yawRateRef}(k))^2 * 2e+4$ ; $J \leftarrow J + (v(k) - vRef(k))^2 * 1e+2$ ; $J \leftarrow J + (u(k) - u(k+1))^* R^* (u(k) - u(k+1))$ ; $J \leftarrow J + vSlack^2 * 1e+7$ ; $J \leftarrow J + leftWheelSlack^2 * 1e+7$ ; $J \leftarrow J + rightWheelSlack^2 * 1e+7$ ;**end for**

---

the objective function is shown in algorithm 2

The weights are designed and tuned to follow the references ( $Q$ ) with respect to different units and measures (yaw rate is in radians thus rather small, velocity in metres per second) and also the fact that no reference on beta or wheel rotation rates is given. The weight matrix  $R$  aims to smoothen the control with giving the objective difference between every control step. The slack weight  $Q_s$  is then, according to theoretical part, significantly larger than the highest weight in the other matrices. This value shall be sufficient based on the fact that the highest another used weight relates to the vehicle's yaw rate.

Last, it is important to note that the controller is supposed to be active all the time, meaning also when the vehicle is accelerating from standstill. The issue is that as the upper  $\omega$  limit is derived from equation 5.17 as

$$\omega_{max} = 1.1 \frac{(v \pm \dot{\psi})}{r}, \quad (5.18)$$

for

$$v = 0 \quad (5.19)$$

the limit is set to zero and the controller's action will be conservative. To solve this issue, a velocity-based switch is implemented inside the controller which, in case when the velocity drops below a certain threshold, uses the low-speed version with non-zero predefined velocity value for omega calculation.



## Chapter 6

### Verification and testing

The control developed in the previous chapter was tested on several models. The first model to test the control on was the most simple, linear model. On top of that, the control was integrated into the nonlinear model for further tuning and testing with open loop driving using inputs from a 'dummy' driver not reflecting the actual driving situation.

The last series of tests were performed in IPG Carmaker [23]. Some tests were performed with an open loop driving, the rest was used with help of closed loop driver. The closed loop driver is collecting the feedback from the vehicle and reacts on the current situation. It is then possible to test how the control would behave when interacting with a driver.

Prior to presenting the results of testing the control, the response of the uncontrolled system is shown for comparison. Since the major difference can be seen in more extreme situations, the tests performed on the split  $\mu$  road are shown in figures 6.1 and 6.2. The figure 6.1 shows how the wheels rotation rates behave since the beginning of the acceleration maneuver. The wheels slip ratios exceeded the limits from the beginning and the ratio grew higher when the vehicle drove on the slippery surface. The yaw rate is then shown in figure 6.2. It is apparent that the driver tried to stabilize the vehicle with a steering wheel as can be seen from the growth of reference.

#### 6.1 Testing with the high fidelity model

First, the tests were performed with the high fidelity model. The structure of the model is shown in figure 6.3. The model consists of the full vehicle

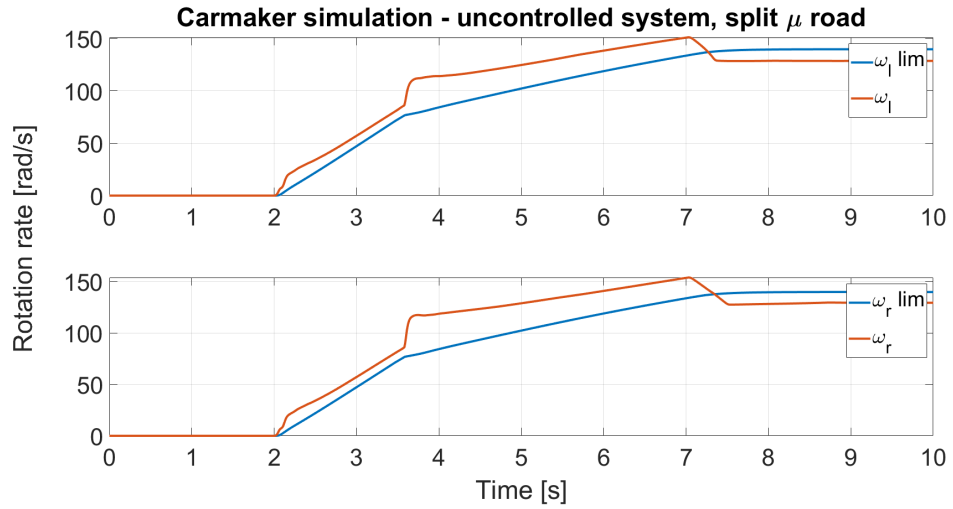


**Figure 6.1:** Wheels rotation rates in uncontrolled simulation setup on split  $\mu$  road

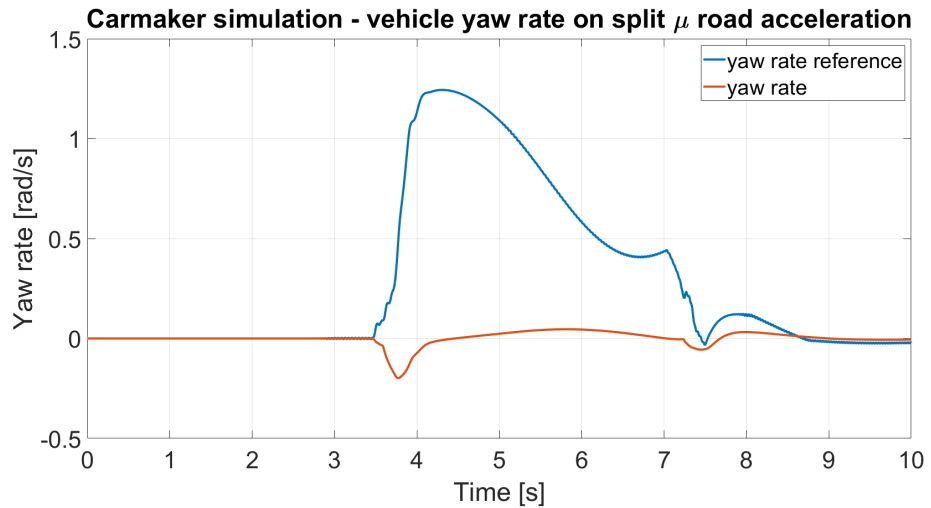


**Figure 6.2:** Yaw rate in uncontrolled simulation on split  $\mu$  road

nonlinear model, the combined TCS and TV MPC implementation, driver's input and a environment modification. The environment is represented by the road  $\mu$  value.

The *TC\_TV\_MPC* block in figure 6.3 contains a Matlab function as Yalmip has no Simulink block implemented. The function inside this block serves only as an interface to the MPC. Its function is to receive the measured data, prepare the state vector and driver's actions and pass it to the MPC. This block also serves as the memory block. It has to remember the previous action taken by the control as it is also a subject for the MPC control. Finally, the control then sends the optimized input values to the vehicle.

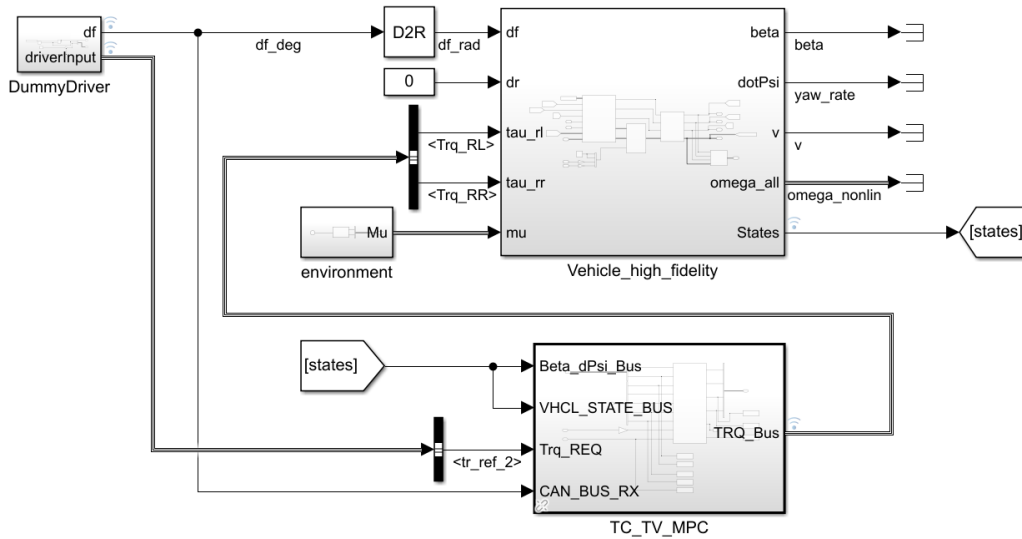


Figure 6.3: Nonlinear model implemented in Simulink

### 6.1.1 Acceleration maneuver

The acceleration maneuver tests the ability of the controller to react on the driver's demand for acceleration. The first two tests, combined together as acceleration and deceleration, are shown in figure 6.4. The vehicle starts with an initial velocity and the driver sets the reference to a higher speed. Then the speed reference is lowered again. As the upper half of the figure shows, the referenced velocity is achieved in both situations, acceleration and deceleration. The lower half shows the applied torque from the controller. The controller kept the torque inside the limit as the motor torque shall never be negative and lower than the motor maximum. The respective wheel rotation rates are shown in figure 6.5 with the upper limit set by the controller. The wheel rates were following the upper limit while accelerating while not exceeding it in any time of the simulation.

The same scenario is then tested again on low split  $\mu$  road to test the performance of the whole system combined. Compared with the normal road, the expectations were met and the acceleration is slower as can be seen in figure 6.6. The lower part of the same figure shows the yaw rate evolution in time. The different road conditions are responsible for the initial change which the controller managed to compensate in time. It is important to note that the controller compensates only the yaw rate disturbances, not potential deviations in yaw angle. It is still expected that the driver will correct them.

The figure 6.7 shows respective rotation rates of the wheels. The change of the surface is intentionally placed in the middle of the acceleration when the controller is holding the wheel rotation rates on the upper limit. The left side, placed on the more slippery surface, was kept on the rotation rate limit

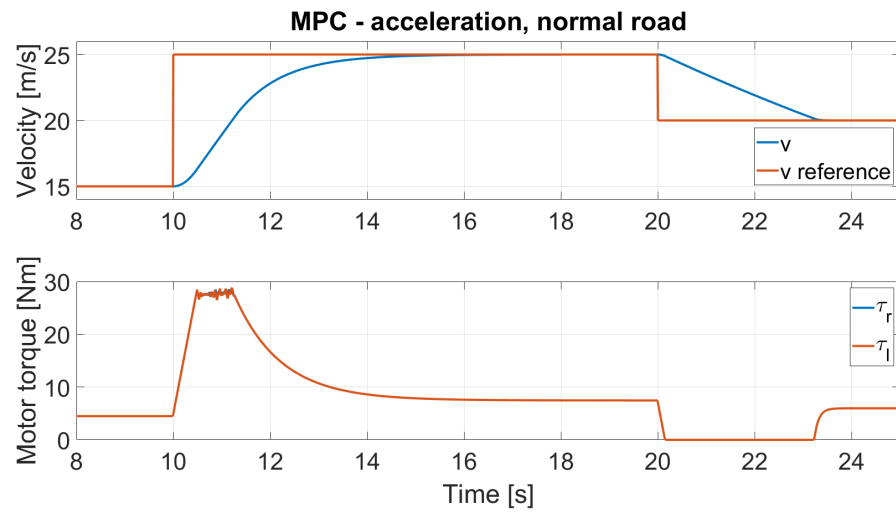


**Figure 6.4:** Response of the controlled system to the acceleration and deceleration. Fluctuations during the acceleration appeared due to reaching omega limit.

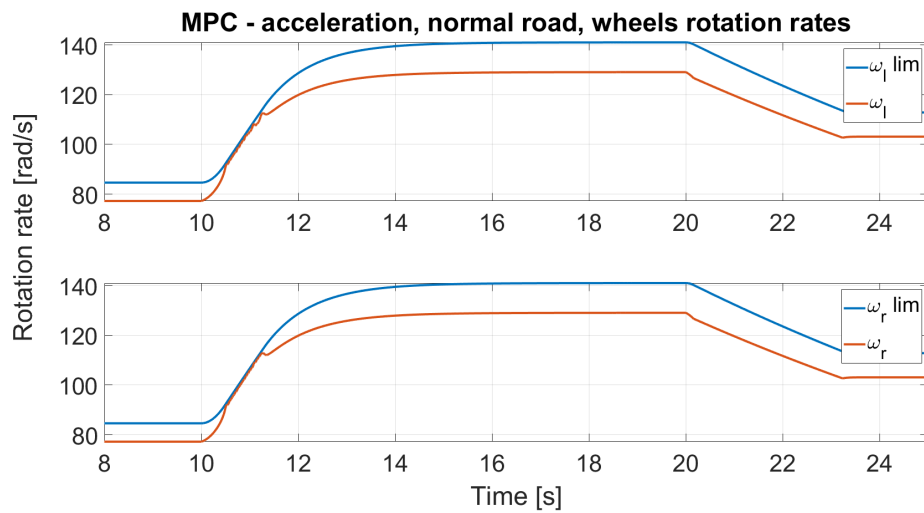


**Figure 6.5:** Response of the controlled system to the acceleration and deceleration; wheel rotation rates. Left wheel rotation rates and limit are displayed in the upper plot, the right in the lower one.

while the right side had a reserve. Comparing the figures 6.6 and 6.7, the cause of this is to drive the yaw rate to zero. The oscillating movement has its origin in not updating the model hence the controller supposes the vehicle is still moving on a regular road. As a result it allows the torques to grow expecting a slower growth of the wheel's rotation rate.

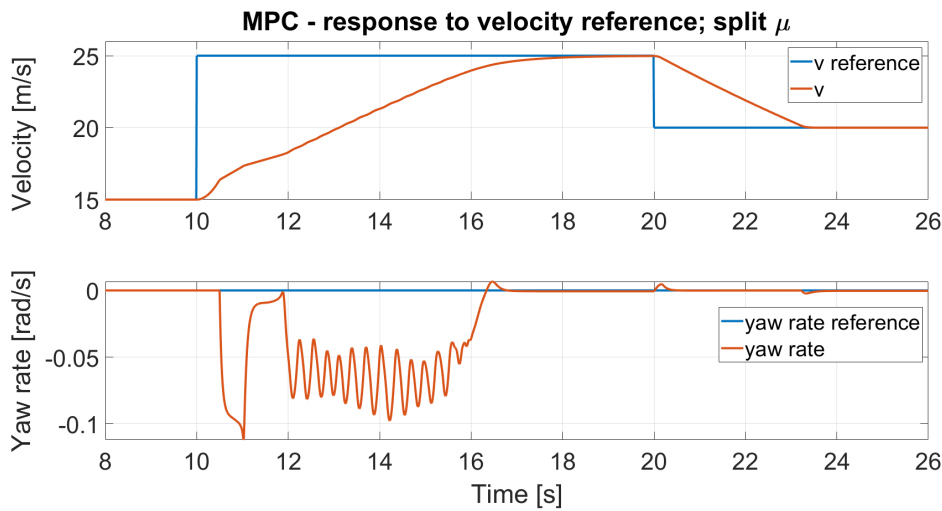


**Figure 6.6:** Response of the controlled system to the acceleration and deceleration on split  $\mu$  road. Upper part displays the left wheel behaviour, the right one is in the lower part.

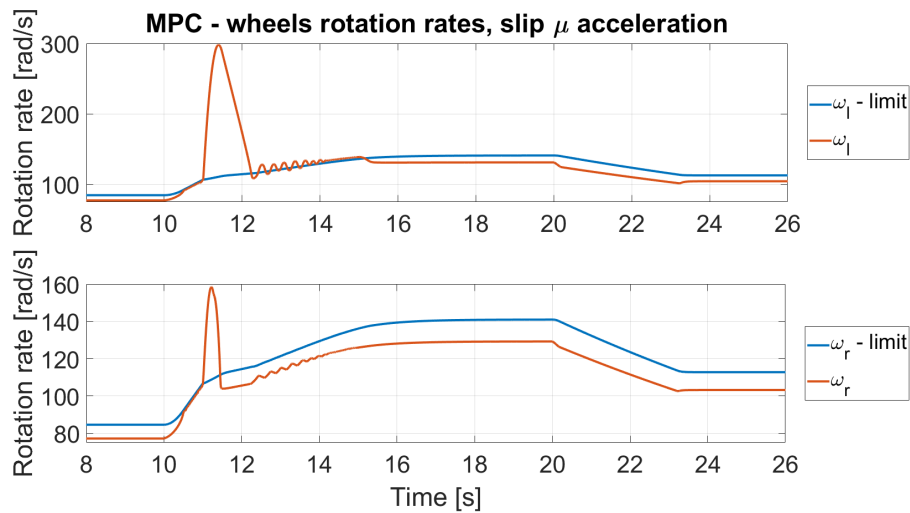


**Figure 6.7:** Response of the controlled system to the acceleration and deceleration on split  $\mu$  road; wheels rotation rates

## 6.1.2 Cornering

The next series of experiments is focused on cornering maneuvers. They are designed to test the controller performance while keeping the original speed or accelerating. Again, the scenarios were tested on a normal road and a low  $\mu$  surfaces. The cornering during acceleration maneuver is shown in figure 6.8. As the steering wheel angle is given as a step input, the yaw rate and its reference grow rapidly. The MPC algorithm lowers the torques and redistributes them to compensate the sudden yaw rate growth.

Figures 6.9 and 6.10 show the results of cornering with acceleration when driving on a low  $\mu$  road. The first of these two figures shows the time evolution of the yaw rate and both applied torques. Again, the step change in the steering wheel angle pushes the yaw rate above the referenced value which the TV part of the controller compensates by lowering the torque on the left motor. Then, after driving onto a slippery part of the road with the left wheel, both torques are lowered in order to prevent excessive slip ratio as shown in figure 6.9. It also shows the controller is able to follow the limit on motor torques difference as they are both lowered synchronously.

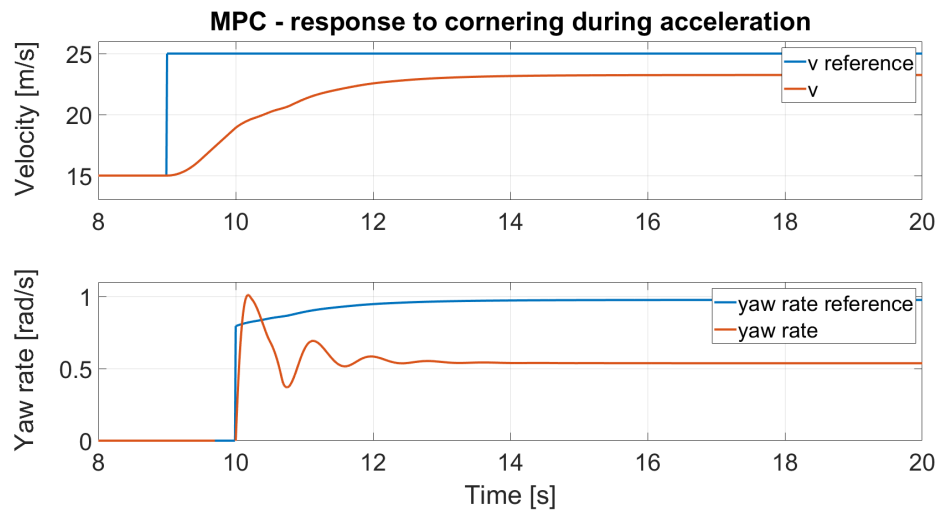


**Figure 6.8:** Response of the system to acceleration and cornering - velocity and yaw rate

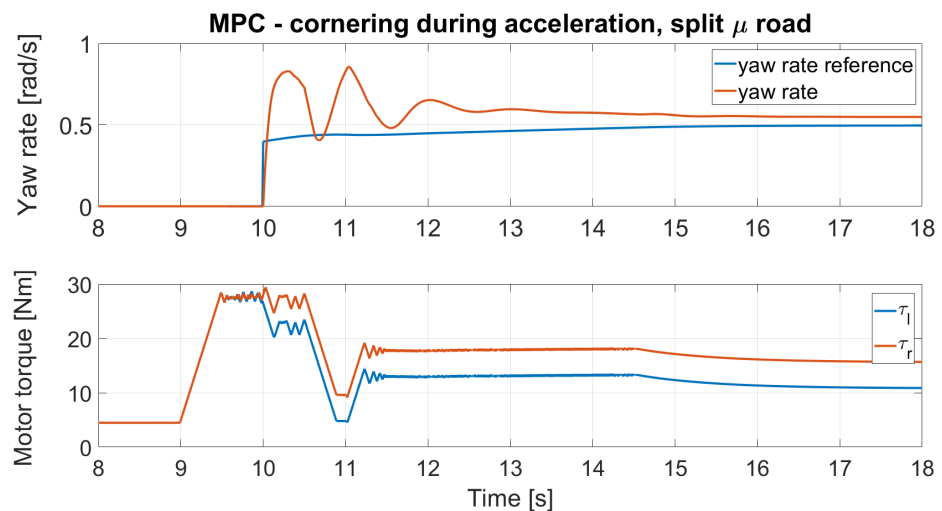


**Figure 6.9:** Response of the system to acceleration and cornering on split  $\mu$  road, yaw rate and torques

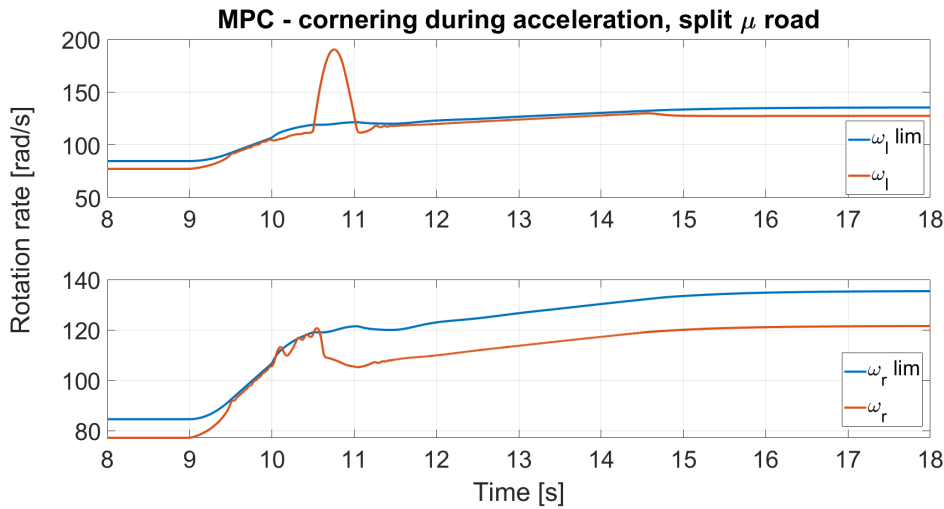


**Figure 6.10:** Cornering during acceleration on split  $\mu$  road, wheels rotation rates for the left wheel in the upper figure, right wheel is in the lower part.

## 6.2 Testing in IPG Carmaker

The second part of the testing was performed in IPG Carmaker [23] with the model which was provided by the CTU e-formula team together with several testing scenarios. Their model of cart-like vehicle on a track can be seen in figure 6.11. The model and simulation in IPG Carmaker is more complex in terms of control and the vehicle behavior. The vehicle motion is no longer only planar, but also other motions are taken into account. The simulation is then enhanced, for example with varying vertical force  $F_z$  based on the driving situation.

Another part of the IPG Carmaker is the full interface to the driver while it still has the possibility to be used as an open loop control with predefined inputs. The driver is able to control the vehicle as if there was a regular person reacting on the current situation. This brings also the necessity to modify the interface as the acceleration pedal signal cannot be used as a velocity reference directly but used for further computation of the reference. For this, a brake pedal signal was incorporated in the calculation of the velocity reference as well. Both signals (acceleration and brake pedal) were then summed and integrated to get the final reference as shown in the figure 6.13. The integrator was also given an upper and a lower limit on the velocity reference.

The control integrated into the Carmaker model can be seen in figure 6.12. Several signals were not included directly in the input buses so the recalculations had to be done for wheels rotation rates and the steering wheel angle. The control is again wrapped inside a Matlab function block serving as an interface between the model and the algorithm.



Figure 6.11: CTU e-formula model in IPG Carmaker

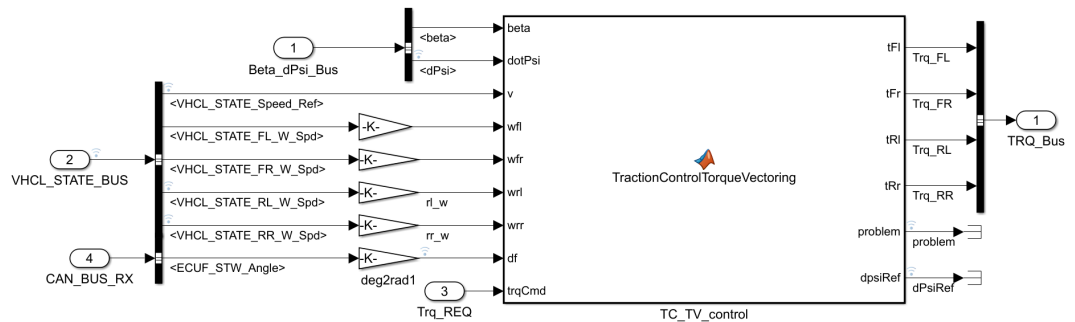


Figure 6.12: Control algorithm integrated into the Carmaker model

### 6.2.1 Acceleration maneuver

The first maneuver to test the control with was the acceleration. As the vehicle starts from standstill, the switch between the two controllers is tested as well. The tests were carried out on a normal road first and then on split  $\mu$ .

The vehicle's velocity and the set reference can be seen in figure 6.15. It is apparent that the acceleration pedal produces a ramp signal instead of the step as it was in the simplified nonlinear model. Compared with figure 6.14 showing the torques from the MPC controller, a spike at approximately about 2.5s is caused by the switch in the control and the controller operates with the actual velocity instead of a 'hard-coded' value for startup. The last figure 6.16 from this test part shows the rotation rates of the wheels. For both wheels their rotation rates were slightly under the given limit. This



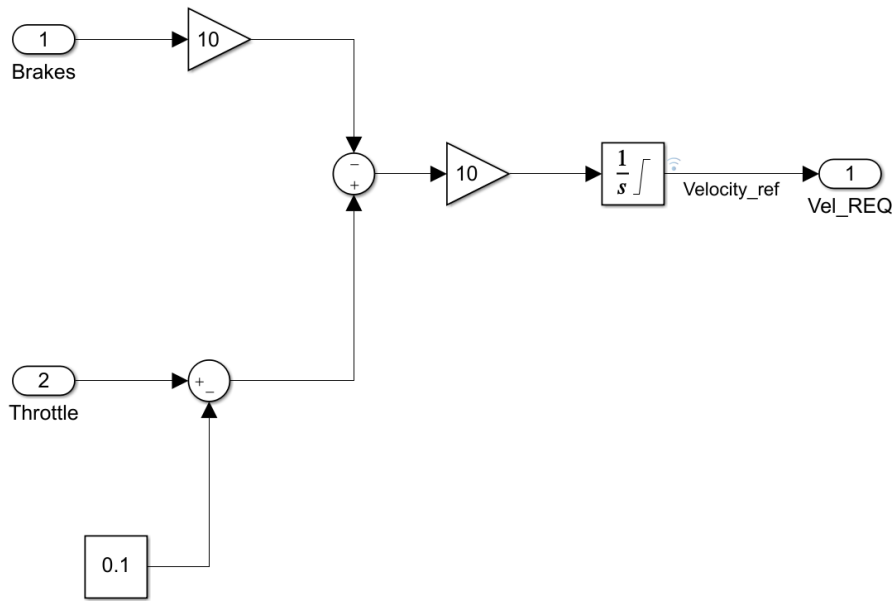


**Figure 6.13:** Velocity reference calculation from brake and acceleration pedal signals

might be caused by inaccuracy of the linear model inside the MPC.

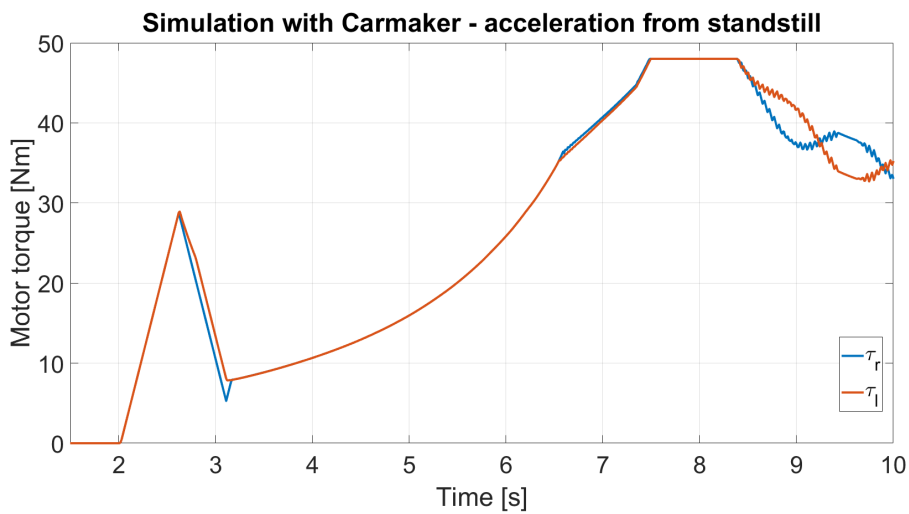


**Figure 6.14:** Motor torques during the acceleration

The next test with acceleration was performed on a split  $\mu$  road. Similar to the nonlinear model testing, the vehicle initially started on a normal road and during the acceleration it drove on different surfaces. The velocity and the vehicle's yaw rate behaviour are shown in figure 6.17. As expected, the acceleration is slower due to less transmittable force. The yaw rate is also driven to zero as the vehicle shall be driving straight. The fluctuations around zero for the yaw rate can be explained with the help of wheels rotation

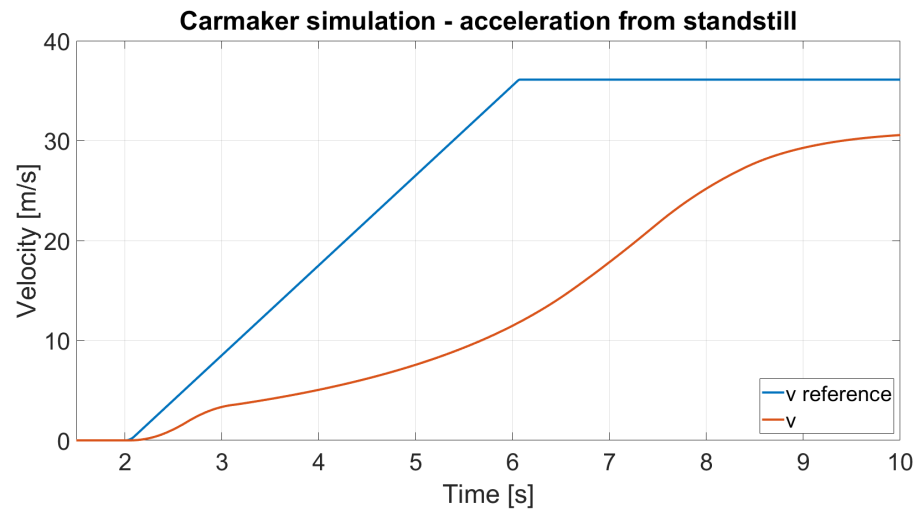


**Figure 6.15:** Controlled system response to acceleration, velocity

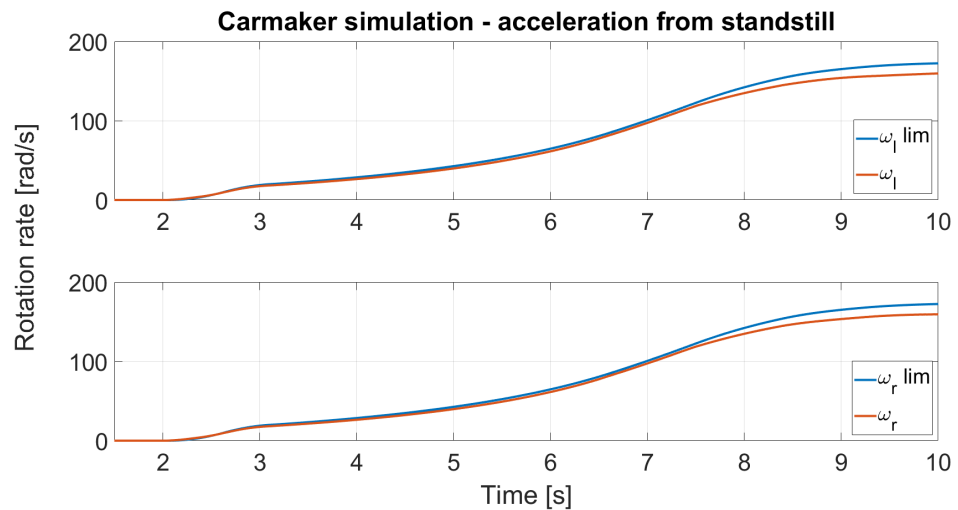


**Figure 6.16:** Controlled system response to acceleration, wheels rotation rates. The left wheel behaviour is in the upper plot, the lower plot is for the right wheel.

rates from figure 6.18. With the inaccuracy of the controller, the MPC is trying to apply more torque on the motors for better acceleration. Lacking the information about the road surface, the wheels keep slipping and the controller lowers the rotation rates to follow the constraints. The different surface type with the contribution of the driver, who is trying to stabilize the vehicle himself, causes the fluctuation. The control however is able to react to changes in both reference and environment.

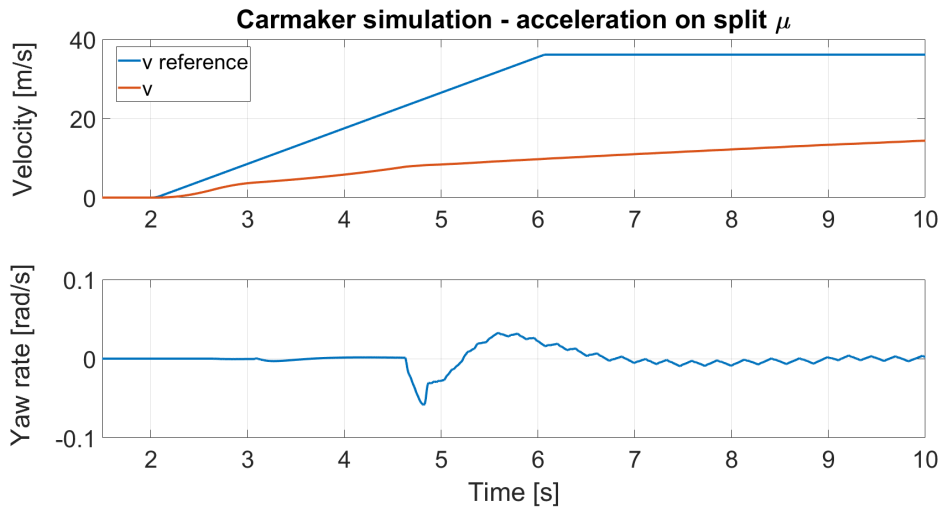


Figure 6.17: Controlled system response to acceleration on split  $\mu$  road

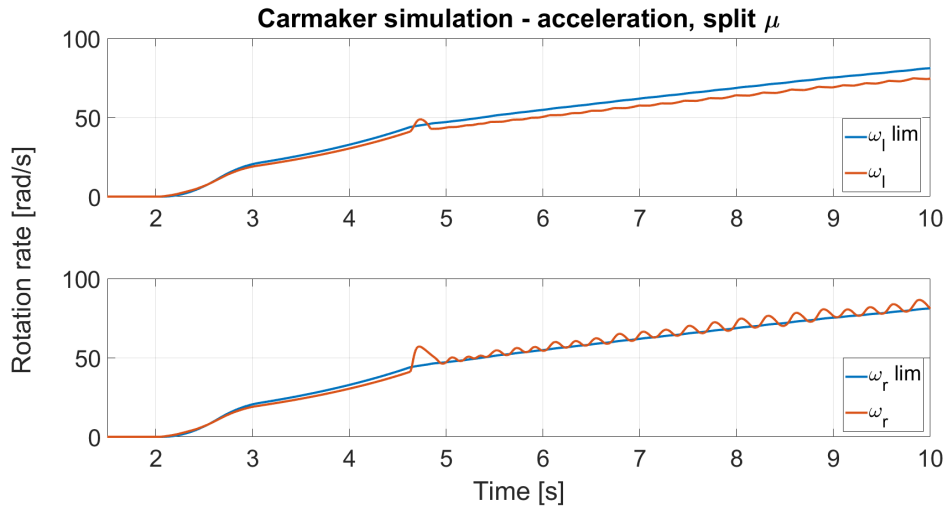
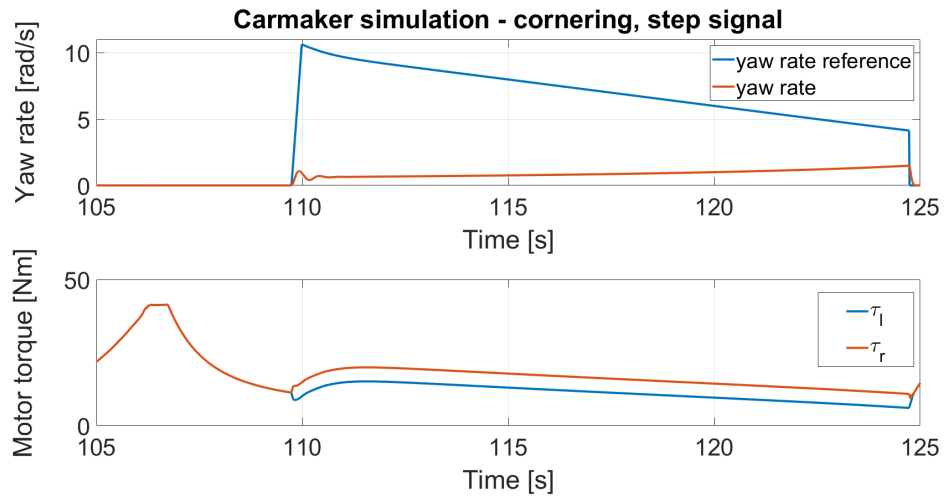


Figure 6.18: Controlled system response to acceleration on split  $\mu$  road, wheels rotation rates - left wheel in the upper plot, right wheel in the lower plot.

## 6.2.2 Cornering

The cornering maneuvers were performed as an open loop test and on a race track. The open loop control scenario contains acceleration to a certain speed, then releasing the acceleration pedal and steering the angle to a certain angle. The figure 6.19 shows that after releasing the gas pedal, the yaw rate reference grew rapidly while the reference is not met and the difference remains significant during the maneuver. This is caused by the limitation of the kinematic equation for the reference. In the lower half of the figure 6.19 the motor torques are displayed. Again, they diverge and follow the limit on the difference as set by the MPC.



**Figure 6.19:** Carmaker simulation results, open loop cornering test

The last part of cornering maneuvers was carried on a simulated test track with the closed loop driver. The idea behind is to test the behaviour of the control in situations close to the real ones. The tests include acceleration from standstill into a turn, a long turn and a maneuver similar to a double lane change. The figure 6.20 shows the torques applied to wheels. The spike again indicates the switch between the startup and the regular driving control. It proved the control to be able to react on the coming requests and distribute the torques to help the vehicle with the maneuver.

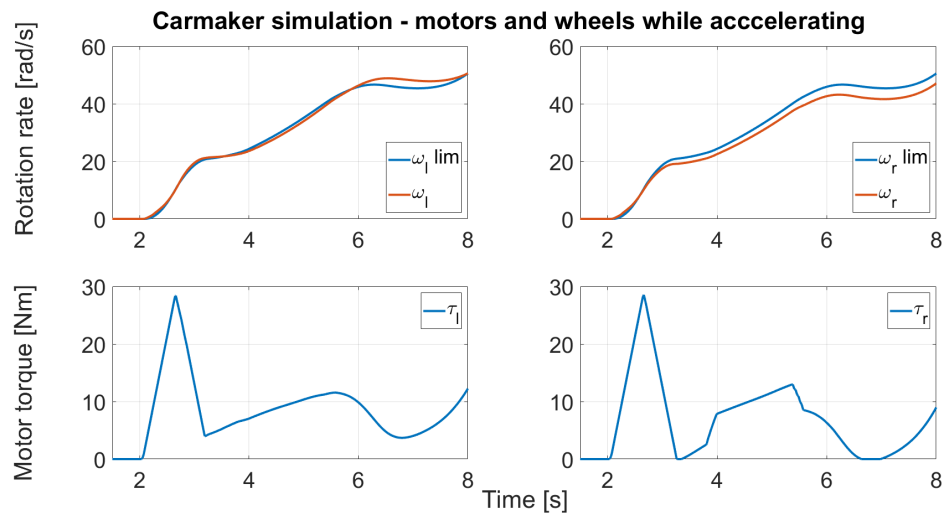


**Figure 6.20:** Simulation of acceleration into a turn

Later on the road, a maneuver similar to a double lane change is performed. It consists of a left turn followed by a right turn and back to straight direction. The vehicle's velocity and yaw rate are shown in figure 6.21. The driver stepped on the brake when changing the directions and then accelerated again.

The torques as distributed in this situation together with the wheels rotation rates are shown in figure 6.22. According to the previous figure, the torques drop together with the velocity reference. At the end of the time window, the beginning of the acceleration can be seen with uneven distribution of the torques.

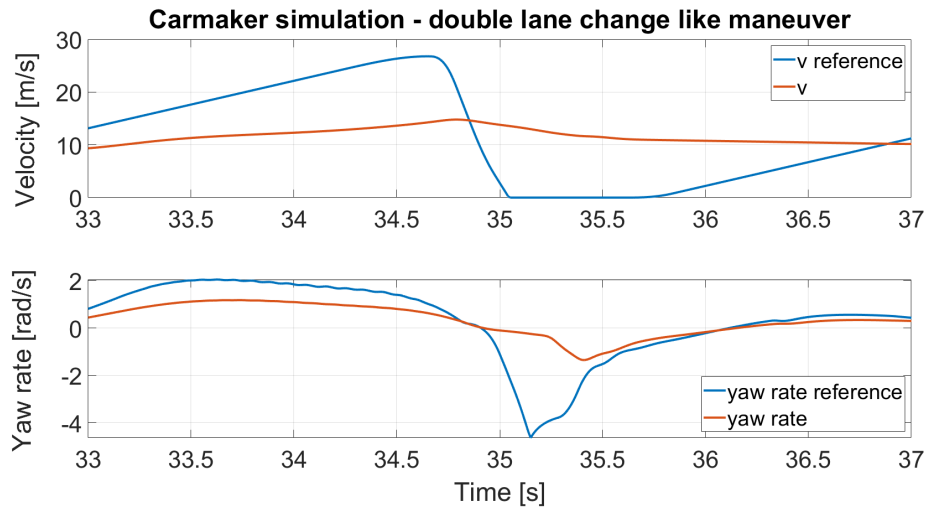


**Figure 6.21:** Simulation of acceleration into a double lane change maneuver, velocity and yaw rate

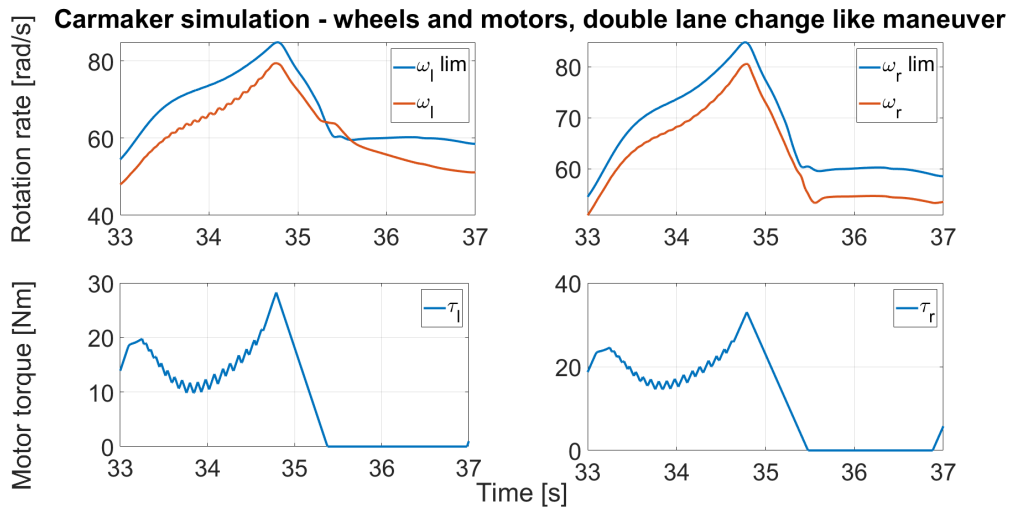


**Figure 6.22:** Simulation of acceleration into a turn, wheels rotation rates and torques

The results of the last performed maneuver are displayed in figure 6.23. The vehicle is accelerating while performing a right turn with a large diameter allowing it to accelerate. The control succeeded and managed to keep the vehicle accelerating while turning. The fluctuations in the yaw rate reference are subject to the automated driving mechanism.

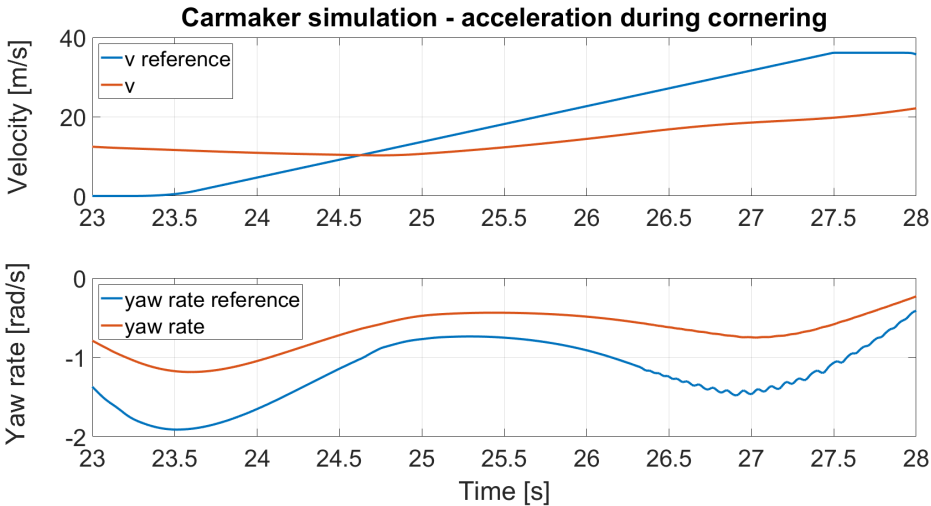


Figure 6.23: Simulation of acceleration into a long turn

## Chapter 7

### Conclusion

#### 7.1 Results

The goal of this thesis, to implement a TCS system combined with a TV system, has been accomplished. The results of the experiments in line with the theoretical research proved that the TV feature is a necessity for the EVs with the same setup as the EV in focus of this thesis (each powered wheel is connected to its own motor). The necessity comes from the fact that this type of EV has no differential unit and the motors have to compensate any difference in the rotation rates of the wheels.

A prototype MPC-based controller was designed, implemented and tested on several different scenarios. Constraints on the control were designed and weights in the system were tuned based on numerous experiments. Based on the presented results, the TCS/TV system is able to react upon sudden changes in the environment and prevent excessive wheel slip ratios while helping the driver to stabilize the vehicle and meeting the requirements defined for the control in the same time.

The requirement for the control real time has not been fully met which is likely to be due to using Yalmip which is rather a prototyping than a production tool. Based on the simulations with the basic linear model using Matlab's profiler, the solver took approximately 17ms for one step calculation.

Overall, the implementation of the TCS and TV is considered to be successful. Still, the implementation leaves space for future work and possible improvements as well as reformulation into a quadratic program. There are many quadratic program solvers which may produce a solution faster thus





## Appendix A

### Bibliography

- [1] PACEJKA, Hans B. *Tyre and Vehicle Dynamics*. Second Edition. Butterworth-Heinemann, 2005. ISBN 9780750669184.
- [2] KIENCKE, Uwe a Lars NIELSEN. *Automotive control systems: for engine, driveline and vehicle*. Berlin: Springer, 2005. ISBN 3-540-23139-0.
- [3] *Automotive handbook*. 7th rev. and expanded ed. Plochingen: Bosch, 2007. ISBN 978-0-8376-1540-0.
- [4] Slash Gear. *Four reasons quad-motor EVs should excite you* [online]. [cit. 2021-8-9]. Available at: <https://www.slashgear.com/four-reasons-quad-motor-evs-should-excite-you-27604474/>
- [5] BMW's iPerformance plug-in hybrid electric vehicle (PHEV) powertrain architecture. *X-Engineering* [online]. [cit. 2021-8-9]. Dostupné z: <https://x-engineer.org/automotive-engineering/vehicle/hybrid/bmw-iperformance-plug-in-hybrid-electric-vehicle-phev-powertrain-architecture/>
- [6] Tesla Model S. *Wikipedia: the free encyclopedia* [online]. San Francisco (CA): Wikimedia Foundation, 2001- [cit. 2021-8-9]. Dostupné z: [https://en.wikipedia.org/wiki/Tesla\\_Model\\_S](https://en.wikipedia.org/wiki/Tesla_Model_S)
- [7] What is Porsche Torque Vectoring? *Porsche Fremont* [online]. [cit. 2021-8-9]. Dostupné z: <https://www.porsche Fremont.com/porsche-torque-vectoring/>
- [8] D. Dogan and P. Boyraz, "Smart Traction Control Systems for Electric Vehicles Using Acoustic Road-Type Estimation," in *IEEE Transactions on Intelligent Vehicles*, vol. 4, no. 3, pp. 486-496, Sept. 2019

- [9] D. A. Aligia, G. A. Magallan and C. H. De Angelo, *EV Traction Control Based on Nonlinear Observers Considering Longitudinal and Lateral Tire Forces*, in IEEE Transactions on Intelligent Transportation Systems, vol. 19, no. 8, pp. 2558-2571, Aug. 2018
- [10] D. Tavernini, M. Metzler, P. Gruber and A. Sorniotti, *Explicit Nonlinear Model Predictive Control for Electric Vehicle Traction Control*, in IEEE Transactions on Control Systems Technology, vol. 27, no. 4, pp. 1438-1451, July 2019
- [11] R. Rajamani, *Vehicle Dynamics and Control*, New York: Springer, 2006. ISBN 0-387-26396-9.
- [12] L. De Novellis, A. Sorniotti and P. Gruber, *Wheel Torque Distribution Criteria for Electric Vehicles With Torque-Vectoring Differentials*, in IEEE Transactions on Vehicular Technology, vol. 63, no. 4, pp. 1593-1602, May 2014
- [13] Salleh, I. & Md zain, M. Z. & Raja, Raja. (2013). Evaluation of Annoyance and Suitability of a Back-Up Warning Sound for Electric Vehicles. International Journal of Automotive and Mechanical Engineering. 8. 1267-1277. 10.15282/ijame.8.2013.16.0104, accessed online on 18.07.2021
- [14] TURNOVEC, Petr. *Vehicle Slip Ratio Control System for Torque Vectoring Functionality* [online]. Prague, 2019 [cit. 2021-8-08]. Available at CTU's digital library. Bachelor thesis. CTU in Prague.
- [15] EFREMOV, Denis. *Unstable ground vehicles and artificial stability systems* [online]. Prague, 2018 [cit. 2021-8-08]. Available at CTU's digital library. Master thesis. CTU in Prague.
- [16] *Our Facilities: Southern Hemisphere Proving Grounds. Southern Hemisphere Proving Grounds* [online]. [cit. 2021-7-29]. Available at: [https://shpg.co.nz/facilities#Hill\\_Gradients](https://shpg.co.nz/facilities#Hill_Gradients)
- [17] *ESP - What is it in?* Punto Marinero [online]. [cit. 2021-8-1]. Available at: <https://cs.puntomarinero.com/esp-what-is-it-in/>
- [18] BEMPORAD, Alberto. *Model Predictive Control* [online]. Lucca [cit. 2021-8-8]. Available at: [http://cse.lab.imtlucca.it/bemporad/teaching/mpc/imt/1-linear\\_mpc.pdf](http://cse.lab.imtlucca.it/bemporad/teaching/mpc/imt/1-linear_mpc.pdf). MPC presentation, doctoral course. School for advanced studies, Lucca.
- [19] Mathworks Helpcenter. *Choose Sample Time and Horizons* [online]. [cit. 2021-8-8]. Available at: <https://www.mathworks.com/help/mpc/ug/choosing-sample-time-and-horizons.html>

- [20] Mathworks: R2020a at a Glance. *Updates to the MATLAB and Simulink product families* [online]. [cit. 2021-8-8]. Available at: [https://www.mathworks.com/products/new\\_products/release2020a.html](https://www.mathworks.com/products/new_products/release2020a.html)
- [21] Löfberg, J., Yalmip. *YALMIP : A Toolbox for Modeling and Optimization in MATLAB* [online]. 2004 [cit. 2021-8-8]. Available at: <https://yalmip.github.io/reference/lofberg2004/>
- [22] Gurobi Optimization. *Gurobi Optimizer* [online]. [cit. 2021-8-8]. Available at: <https://www.gurobi.com/products/gurobi-optimizer/>
- [23] IPG Automotive. *CarMaker: Virtual testing of automobiles and light-duty vehicles* [online]. [cit. 2021-8-8]. Dostupné z: <https://ipg-automotive.com/products-services/simulation-software/carmaker/>





## **Appendix B**

### **Project specification**

## I. Personal and study details

Student's name: **Valerián Jakub** Personal ID number: **457238**  
Faculty / Institute: **Faculty of Electrical Engineering**  
Department / Institute: **Department of Control Engineering**  
Study program: **Cybernetics and Robotics**  
Branch of study: **Cybernetics and Robotics**

## II. Master's thesis details

Master's thesis title in English:

**Advanced traction system development**

Master's thesis title in Czech:

**Návrh pokročilého trakčního systému vozu**

Guidelines:

Multi-engine vehicle platforms start to be the norm in the automotive industry these days. The traction system configuration with two engines per axle enables advanced traction control concepts, providing higher vehicle maneuverability and active safety. The advanced traction algorithm implementing antisymmetric traction torque distribution will be developed and tested in this thesis. The following points will be addressed:

1. Get familiar with vehicle dynamics and traction system concepts.
2. Implementation of vehicle twin-track high fidelity model suitable for torque vectoring.
3. Development of traction control system based on advanced control strategies.
4. Verify traction control system performance.

Bibliography / sources:

- [1] Dieter Schramm, Manfred Hiller, Roberto Bardini – Vehicle Dynamics – Duisburg 2014
- [2] Hans B. Pacejka - Tire and Vehicle Dynamics – The Netherlands 2012
- [3] Robert Bosch GmbH - Bosch automotive handbook - Plochingen, Germany : Robet Bosch GmbH ; Cambridge, Mass. : Bentley Publishers
- [4] Rajamani R. - Vehicle Dynamics and Control, ISBN 978-1-4614-1432-2, Springer, London

Name and workplace of master's thesis supervisor:

**doc. Ing. Tomáš Haniš, Ph.D., Department of Control Engineering, FEE**

Name and workplace of second master's thesis supervisor or consultant:

Date of master's thesis assignment: **26.01.2021** Deadline for master's thesis submission: **13.08.2021**

Assignment valid until:

**by the end of winter semester 2022/2023**

\_\_\_\_\_  
doc. Ing. Tomáš Haniš, Ph.D.  
Supervisor's signature

\_\_\_\_\_  
prof. Ing. Michael Šebek, DrSc.  
Head of department's signature

\_\_\_\_\_  
prof. Mgr. Petr Páta, Ph.D.  
Dean's signature

## III. Assignment receipt

The student acknowledges that the master's thesis is an individual work. The student must produce his thesis without the assistance of others, with the exception of provided consultations. Within the master's thesis, the author must state the names of consultants and include a list of references.

\_\_\_\_\_  
Date of assignment receipt

\_\_\_\_\_  
Student's signature



## **Appendix C**

### **CD Contents**

## Content of the CD:

### Compressed folder:

- data
  - **eformula\_dataset.mat**: dataset for the MPC usage with formula parameters
- model
  - **lib.slx**: library with the controllers
  - **high\_fidelity\_model.slx**
- Scripts
  - **linearization**: linearization tool
  - **TC\_TV\_control.m**: MPC controller function
  - **TC\_TV\_control\_startup.m**: MPC controller function, used for standstill acceleration
- **setupScript.m**: script for simulation setup, linear model generation and basic simulation